

University of KwaZulu-Natal

*Sub transmission Insulator and Conductor Ageing in Coastal
Environments*

Ashwin Ramsoomar

Master's in science in Electrical Engineering

Durban, 2022

*Sub transmission Insulator and Conductor Ageing in Coastal
Environments*

by

Ashwin Ramsoomar

Student No:218088116

*In fulfilment of Master of Science in Engineering, College of Agriculture, Engineering and Science,
University of KwaZulu-Natal*

July 2022

Supervisor: Dr A Swanson

Declaration

I, Ashwin Ramsoomar, hereby declare that the thesis entitled “*Sub transmission Insulator and Conductor Ageing in Coastal Environments*” is my own unaided work, that has not been submitted in fulfilment for any degree or examination in any other university. All sources that were consulted or quoted have been acknowledged in the text and listed in the referencing.

Signature.....

Date..... 16 February 2023

Declaration - Plagiarism

I, Ashwin Ramsoomar, declare that:

1. The research reported in this thesis, except where otherwise indicated, is my original research.
2. This thesis has not been submitted for any degree or examination at any other university.
3. This thesis does not contain other persons’ data, pictures, graphs, or other information, unless specifically acknowledged as being sourced from other persons.
4. This thesis does not contain other persons' writing, unless specifically acknowledged as being sourced from other researchers. Where other written sources have been quoted, then:
 - a. Their words have been re-written, but the general information attributed to them has been referenced.
 - b. Where their exact words have been used, then their writing has been placed in italics and inside quotation marks and referenced.
5. This thesis does not contain text, graphics or tables copied and pasted from the Internet, unless specifically acknowledged, and the source being detailed in the thesis and in the Bibliography section.

Signed

Ashwin Ramsoomar

.....

As the candidate's Supervisor I agree/do not agree to the submission of this thesis.

Signed

Andrew Swanson



Acknowledgements

The following people/ organizations need acknowledgement for their contribution to the culmination of this report, namely:

- GOD.
- **Eskom Holdings KZN Operating Unit** for allowing a study of this type inclusive of release of information.
- **Family (Nitasha, Rohan & Sejl)** for continued support and allowing me the time to pursue my dreams.

Abstract

Globally, power grids are gradually unbundling to encourage multiple sources of small to medium scale renewable generation, aiding in relieving demanding power constraints [1]. The additional generation product requires an effective and efficient power evacuation system; however, the constrained transmission and sub transmission systems are burdened with the higher power transfer limits coupled with aged infrastructure. Operations and maintenance strategies assist in alleviating the temporary system load increases; however, an asset management strategy is required to ensure that the power system operates at a peak without encouraging a redesign or replacement of the entire power system [2]. The guiding principles of an asset management strategy is understanding the effective utilization of sub systems and components. Effective utilization of components can only be achieved, once a useful lifespan is determined, replacing, refurbishing, or instituting life extension measures once the component end of life is neared. To avert underutilizing or overutilizing the asset, the asset age base needs to be determined incorporating in-situ conditions to provide a reliable and generic prediction model.

In sub transmission and transmission systems, maintenance funding, is allocated to critical components such as insulators, ACSR phase conductor and galvanized steel shield wire. These high failure-impact components are susceptible to a higher rate of corrosion related failure, attributed to environmental conditions such as high humidity and high air contamination found in coastal environments. The corrosion models guided by ISO 9223 [3], makes use of empirical degeneration rates for Aluminium, Steel and Zinc. These models understate the initiation of the corrosion reaction for the first year only, requiring the derivation of an acceleration model to represent the degeneration of the composite conductor over its lifespan. The resulting model predicts the useful life of the conductor by measuring the loss in tensile strength attributed to corrosion. Age prediction modelling of the silicone composite insulator is achieved by predicting the loss of creepage or resistive layer on the insulator surface. The coastal environmental conditions, contribute significantly to degenerating the resistive layer leading to a flashover at line voltage. The validation of the insulator and conductor ageing models are achieved by comparing the calculated lifespans to measured field-samples tests. The results showed a standard deviation of 4 years between the measured and calculated values.

Contents

| | |
|--|-------------|
| DECLARATION | III |
| ACKNOWLEDGEMENTS | V |
| ABSTRACT | VI |
| DEFINITIONS | VIII |
| ABBREVIATIONS | IX |
| LIST OF FIGURES | X |
| LIST OF TABLES | XI |
| CHAPTER 1 INTRODUCTION | 1 |
| 1.1 THE RESEARCH PROBLEM | 1 |
| 1.2 RESEARCH OBJECTIVES | 2 |
| 1.3 METHODOLOGY | 3 |
| 1.4 CHAPTER ORGANISATION | 4 |
| 1.5 SUMMARY | 5 |
| CHAPTER 2 LITERATURE REVIEW | 6 |
| 2.1 INTRODUCTION | 6 |
| 2.2 ASSET MANAGEMENT PRINCIPLES | 6 |
| 2.3 INSULATOR AGEING | 8 |
| 2.3.1 Insulator Properties | 9 |
| 2.3.2 Contamination Flashover | 12 |
| 2.4 PHASE CONDUCTOR AND SHIELD WIRE AGEING | 16 |
| 2.4.1 Properties of Phase Conductor and Galvanized Steel Shield wire | 17 |
| 2.4.2 Corrosion Types | 19 |
| 2.4.3 Corrosion Ageing | 20 |
| 2.4.4 Corrosion Failure Probability | 23 |
| 2.5 SUMMARY | 25 |
| CHAPTER 3 MODELLING AND ANALYSIS | 26 |
| 3.1 INTRODUCTION | 26 |
| 3.2 INSULATOR CONTAMINATION FLASHOVER MODELLING | 26 |
| 3.2.1 Accelerated Ageing Factor Insulators | 28 |
| 3.2.2 Insulator Ageing Model Validation | 32 |
| 3.3 CONDUCTOR AND SHIELD WIRE CORROSION MODELLING | 34 |
| 3.3.1 Accelerated Ageing Factor Conductor and Shield wire | 36 |

| | | |
|----------------------------------|---|-----------|
| 3.3.2 | Conductor Ageing Model Validation..... | 40 |
| 3.3.3 | Shield Wire Ageing Model Validation | 44 |
| 3.4 | SUMMARY | 48 |
| CHAPTER 4 CONCLUSION..... | | 49 |
| BIBLIOGRAPHY..... | | 52 |

Definitions

| | |
|--|--|
| All Aluminium Alloy Conductor (AAAC) | Refers to conductor that is composed of an aluminium alloy combining qualities of relatively good conductivity, high tensile strength, and superior corrosion resistance. |
| Aluminium Conductor Steel Reinforced (ACSR): | Refers to conductor with aluminium outer layers and inner galvanised steel core. The outer strands of high-purity aluminium provide good conductivity, low weight, low cost while the inner steel strands provide tensile strength |
| All Aluminium Conductor (AAC) | Refers to conductor that has high conductivity with moderate strength, offering good corrosion resistance with low weight to strength capabilities. |
| Arcing distance | Refers to the shortest external air path around the insulator for a normal and fault operating voltages, to flow to earth. This distance defines the minimum length to prevent power frequency and impulse flashovers. |
| Asset Management | Refers to a systematic coordinated activity or practice through which a utility optimally manages its assets. Objectives are to manage asset performance, risks, and expenditures over their life cycle as per strategic plan. |
| Creepage Distance | Refers to the shortest distance/s along the sheds of the insulator, between the live and dead-end fitting, also referred to as the leakage distance. |
| Dry-arcing distance | Refers to the shortest distance through the surrounding medium between terminal electrodes, or the sum of the distances between intermediate electrodes, whichever is shorter. |
| Economic lifetime | Refers to the economic value of equipment in terms of asset management. The economic lifetime of an asset may extend |

| | |
|-----------------------------|--|
| | or shorten the lifespan of the asset based on the costs associated in running that asset. |
| Expected Useful Life | Refers to the extent of an asset’s life, in which it can comply technically and economically within the prescribed minimum standards. |
| Flashover | Refers to a disruptive discharge across the insulator between those parts of the insulator that normally have the operating voltage between them. |
| Hydrophobic/ Hydrophobicity | Refers to the resistance of a material (silicone), to the formation of water droplets on the insulator surface. |
| Natural ageing | Refers to environmental and operational deterioration after a period of operation. These ageing effects do not consider abnormal failure events in the ageing process. |
| Pitting Corrosion | Refers to localised corrosion that occurs on specific places on a metal substrate, forming a depression or “pit” as a result of loss of material. This corrosion occurs as a result of an electrolytic reaction. |

Abbreviations

| | |
|------|------------------------------------|
| AHI | Asset Health Index |
| AHT | Alumina Trihydrate |
| CBM | Condition Based Maintenance |
| EPDM | Ethylene Propylene Diene Monomer |
| ESDD | Equivalent Salt Deposition Density |
| EVA | Ethylene Vinyl Acetate |
| HTV | High Temperature Vulcanised |
| LSR | Liquid Silicone Rubbers |
| PDMS | Polydimethylsiloxane |
| UTS | Ultimate Tensile Strength |

List of Figures

| | |
|---|----|
| Figure 1-1 Proposed process flow for ACSR conductor and Steel Shield wire lifespan modelling | 3 |
| Figure 1-2 Proposed process flow for Composite Insulators lifespan modelling | 4 |
| Figure 2-1 Basin curve representing the failure rate of equipment | 7 |
| Figure 2-2 Structure of a composite insulator | 10 |
| Figure 2-3 $U_{50\%}$ Voltage for 132kV insulator with varying rain flow rates in an E5 contamination environment..... | 13 |
| Figure 2-4 Probability distribution function showing the risk of flashover[36]..... | 16 |
| Figure 2-5 Cross Sectional view of a 4-layer ACSR conductor | 17 |
| Figure 2-6 Aluminium strand strength (1350-H19) utilised for ACSR conductor..... | 18 |
| Figure 2-7 Galvanised Steel wire strand strength for Class A galvanised Steel wire | 18 |
| Figure 2-8 Corrosion effect of sodium chloride concentration on iron | 21 |
| Figure 2-9 Sulphur dioxide concentration map of South Africa [75]. | 22 |
| Figure 2-10 Corrosion loss over the material lifespan. (a) Taman (1923) for atmospheric corrosion, (b) Melchers multi-mode corrosion process,(c) Marine and atmospheric corrosion [83] | 24 |
| Figure 2-11 Various stages of corrosion in a multi-layered model..... | 24 |
| Figure 3-1 Obenaus adapted model of contaminated insulator | 26 |
| Figure 3-2 Insulator Accelerated Ageing model (13 years)..... | 30 |
| Figure 3-3 Insulator Accelerated Ageing model (50 years)..... | 30 |
| Figure 3-4 Surface resistance degeneration over a period of time | 31 |
| Figure 3-5 Flashover lifespan prediction for 132kV silicone insulator in E1-E7 contamination categories..... | 32 |
| Figure 3-6 Predicted vs Measured insulator failures | 33 |
| Figure 3-7 The standard deviation for the calculated flashover values..... | 34 |
| Figure 3-8 ACSR conductor Accelerated Ageing model (18 years) | 37 |
| Figure 3-9 ACSR conductor Accelerated Ageing model (100 years) | 38 |
| Figure 3-10 Shield wire Accelerated Ageing model (30 years) | 39 |
| Figure 3-11 Shield wire Accelerated Ageing model (100 years) | 40 |
| Figure 3-12 Graphical representation of first year Aluminium strand loss for Wolf ACSR conductor samples | 41 |
| Figure 3-13 First year corrosion rate of Wolf and Bear samples | 42 |
| Figure 3-14 Calculated UTS loss for Wolf and BEAR samples | 43 |
| Figure 3-15 Measured and calculated age of Wolf and Bear samples | 43 |
| Figure 3-16 Standard deviation plot between measured and calculated life prediction | 44 |
| Figure 3-17 Loss of galvanizing on the outer cores of the various shield wires for the first year | 45 |
| Figure 3-18 Loss of galvanizing on the outer cores of the various shield wires | 46 |
| Figure 3-19 Calculated UTS loss for the various shield wire samples | 46 |
| Figure 3-20 Variance between the calculated and measured age prediction of the various shield wires..... | 47 |
| Figure 3-21 Standard deviation plot between the calculated and measured shield wire samples..... | 47 |

List of Tables

| | |
|---|----|
| Table 2-1 Prescribed minimum lifespan of electrical equipment according to NRS 093-1 | 8 |
| Table 2-2 Various site severity classes based on ESDD and DDDG measurements in South Africa (2001-2005) and IEC 60815-1 | 14 |
| Table 2-3 Changes in Air Pressure & Relative Density with Altitude | 15 |
| Table 2-4 Global studies of salt deposition daily rates | 21 |
| Table 2-5 Potential sulphur dioxide levels generated from various sources..... | 22 |
| Table 2-6 Wetness classification based on time of wetness. | 23 |
| Table 3-1 Insulator failure data used to calculate the Ageing Acceleration factor | 29 |
| Table 3-2 Flashed insulators and distance from contamination source..... | 32 |
| Table 3-3 Data for the insulator lifespan variance calculation | 33 |
| Table 3-4 Data for the conductor Ageing Acceleration calculation..... | 37 |
| Table 3-5 Data for the conductor Ageing Acceleration calculation..... | 39 |
| Table 3-6 Data used for the first year Aluminium strand area loss calculation, for Wolf ACSR conductor samples.. | 41 |
| Table 3-7 Data used for the first year Galvanised Steel strand material loss calculation | 45 |

CHAPTER 1 INTRODUCTION

The advanced research and development into the field of electro-thermal-mechanical stress modelling, have been a key contributor to electrical component ageing and prediction models. Understanding the modes of failures, has paved the path for compact, economical, and innovative components design across various sectors of the power system. The results of design improvements are cascaded into enhanced system performance, allowing asset managers to reap the benefit of the improved component life. However, eventually all components and systems age, resulting in constant failures and poor performance. It is of importance to asset managers to fit the failure rates into an ageing profile for specific components. The ageing profile can be utilised to financially motivate for the asset replacement, refurbishment, or retirement [4].

In the electrical power transmission and sub transmission system, component failures have a significant impact on the delivery of energy to the customers, utilities, and power producers. The cost of unserved energy has economic as well as reputational implications, requiring adequate measures be established in insuring that the systems perform optimally [5]. Sub transmission systems are composed of towers that mechanically support conductor, transferring power from a transmission substation to a distribution substation, generally several kilometres apart. The failure of single insulator or piece of conductor, may disable the system for hours if not days, highlighting the importance of understanding and planning for such events. Sporadic or uncontrolled events that impact the line can be managed, however component failure prediction and component ageing is a key requirement to asset and operational managers [6].

1.1 The Research Problem

The application of asset management principles [7] on sub transmission systems require implicit and proficient understanding of systems and components for the various failure and ageing categories. In the analysis of individual components, a segregation is required for critical and non-critical components. The criticality, which is measured on the impact of failure and failure frequency, results in the conductor and insulator being the highly prioritized as critical components.

The failure of silicone composite insulators is confined to two modes mainly, the first being flashover as a result of lightning activity and the second, is failures related contamination flashovers. Lightning activity results in the failure of the insulator, which is not necessarily attributed to the natural ageing of the insulator. Unlike contamination related flashovers, the gradual loss of the resistive lay on the insulator surface results in a flashover. The main contributor to the loss of the resistive layer especially in coastal environments, are the effect of environmental conditions such as wetness, temperature, and contaminants. The problem that most asset managers are faced with, is determining the is the useful life of silicon composite insulators in especially in coastal environments.

Similarly, ACSR conductor and shield wire are susceptible to electrical and mechanical stresses, electrical stresses are mainly mitigated against by protection circuits that ensure the excess current above recommended, and short circuit faults, are limited. The mechanical stresses, however, cannot be so easily negated. Environmental factors such as high wetness, temperature and contaminants combine to erode the conductor surface material, thereby reducing the tensile strength of the conductors. The problem arises where asset managers are required to predict the useful life of ACSR and shield wire conductor, incorporating environmental conditions such as wetness, temperature, and contaminants.

The research problem is to determine the useful life of sub transmission silicon composite insulators, ACSR conductor and steel shield wire that are exposed to coastal environmental conditions.

1.2 Research Objectives

Material degeneration as a result of harsh environmental conditions, can reduce the mechanical or electrical life of sub transmission line components. Generic life prediction models provide an estimate of the useful life of a component based on minimal available information, however in cases where site condition-based information is available, a tailored life prediction model should be investigated. Therefore, the research objectives are to investigate, model, and validate the lifespan of electrical components of a sub transmission line, tailored to the available environmental information. These objectives are listed in the following research questions namely:

- a) To investigate the effect of wetness, temperature, and contaminants in reducing the lifespan of
 1. ACSR conductor.
 2. Galvanised steel shield wire.
 3. Silicon composite insulators.
- b) To determine the resulting correlation between these three parameters must be tested against field samples in a form of a component degeneration model.

The empirical study will make use of material degeneration rates that have produced by the International Standards Organization (ISO) and accepted by industry. These degeneration rates that are mainly applicable to Steel, Aluminium and Zinc will be validated and applied to a multi core, multi layered phase conductor and shield wire. The degeneration rates for the conductor and shield wire will be translated into mechanical strength and validated against in-situ samples. Insulator ageing will concentrate on the process of contamination flashover at normal operating voltage using empirical analysis of defined linear regression flashover models. Once the theoretical parameters of the ageing models are established, the model will be validated against case studies of insulator failures.

1.3 Methodology

The empirical study will make use of material degeneration rates that have produced by the International Standards Organization (ISO) and accepted by industry. These degeneration rates that are mainly applicable to Steel, Aluminium and Zinc will be validated and applied to a multi core, multi layered phase conductor and shield wire. The degeneration rates for the conductor and shield wire will be translated into mechanical strength and validated against in-situ samples [8]. The process flow is shown in figure 1-1. Insulator ageing will concentrate on the process of contamination flashover at normal operating voltage using empirical analysis of defined linear regression flashover models. Once the theoretical parameters of the ageing models are established, the model will be validated against a case study of insulator. The process flow is shown in figure 1-2.

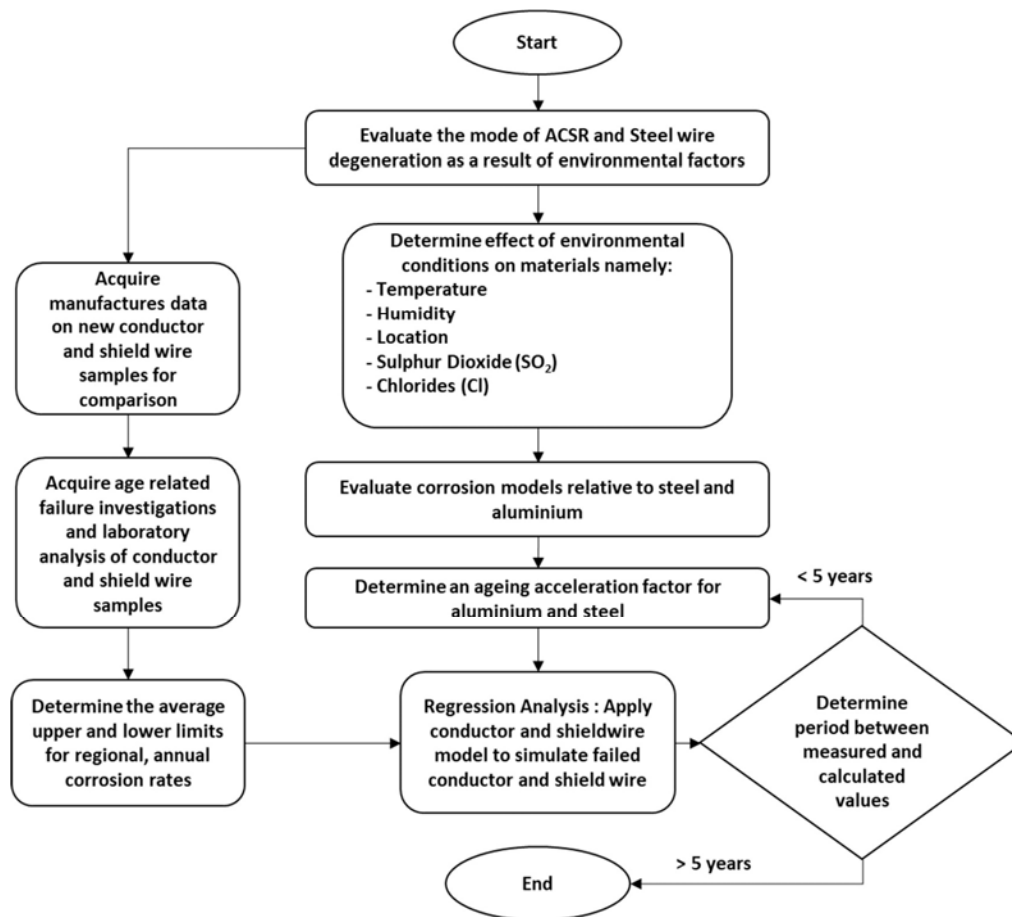


Figure 1-1 Proposed process flow for ACSR conductor and Steel Shield wire lifespan modelling

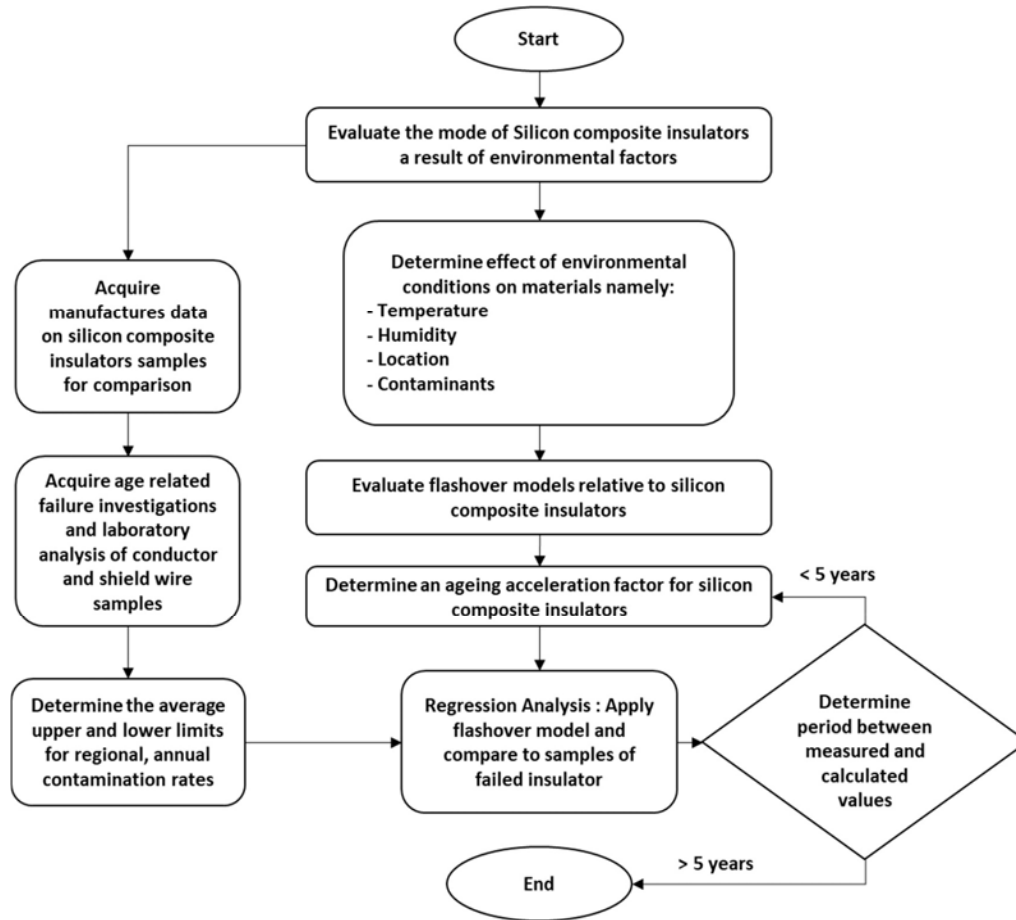


Figure 1-2 Proposed process flow for Composite Insulators lifespan modelling

1.4 Chapter Organisation

The layout of the dissertation follows a methodical approach to establish a foundation and bearing of the research in both academia and industry. It comprises of four chapters, each constructed on the previous chapter aiming to fulfil the objectives set forth. A summary of the chapters is previewed below, namely

- Chapter 1: The research topic is introduced, instigating the need for asset management research, in the electrical power industry. Sub transmission lines are highlighted as the focus area of study, followed by the research objectives which focus on the lifespan prediction of insulators and conductors. Thereafter, the methodology utilized in the study is discussed and the chapter concludes with a summary.
- Chapter 2: The literature review investigates asset management practices and reinforces the need to understand component behaviour to allow for effective spending. Insulator, conductor, and shield wire fundamentals are reviewed, and emphasis is placed on the environmental conditions that are the main source of its degeneration.

- Chapter 3: The modelling is achieved by applying the empirical evaluations for material degeneration, defining the effect that corrosion has on shield wire and phase conductor degeneration. Insulators degeneration is investigated with a firm focus on the contribution of environmental conditions. The chapter is concluded by correlating the calculated lifespan predictions to in-situ failures, both for conductor and insulators.
- Chapter 4: The concluding chapter highlights the findings and possible reasons to the variance in calculated and measured results. Additionally, the aim of the research is validated to determine if it was achieved by the information presented.

1.5 Summary

Asset management principles warrants the need into system and component ageing research, especially in the electrical power industry where component failure may result in loss of life. Ageing behaviour of insulators, conductor and shield wire forms the basis for the research, with a focus on the effects of coastal environmental conditions on these components. The research methodology implemented to answer the research objectives, make use of empirical equations that have been pre-investigated by the ISO for conductor and shield wire modelling. Insulator related age modelling follows a similar process to that of conductor and shield wire, where empirical equations are applied to arrive at a useful lifespan, where all three models are validated against in-situ failures. A process flow is highlighted both for conductor and insulators, to establish a roadmap for the research. The chapter organization provides a framework for the presentation of information.

CHAPTER 2 LITERATURE REVIEW

2.1 Introduction

Asset Management philosophies recognised in PAS 55, requires the establishment of benchmarked component lifespan for effective asset management. Sub transmission lines are composed of several individual components, some providing mechanical support and others providing both electro-mechanical functions. Towers or structures may be available in a wide variety of shapes and sizes, composed of wood, steel or composite materials, each performing the equivalent functions of supporting the power carrying conductor. Self-supporting lattice steel structures, were predominantly utilized in the 1930-2000 in South Africa, gradually expanding to steel monopoles and guyed steel structures. Structures, foundations, and attachment hardware failure are infrequent as compared to insulator shield wire and conductor failures. This is attributed to the robust designs, which incorporate higher margin of safety or high redundancy margin for various installation applications. Additionally, towers are designed to accept a variety of conductor, shield wire and insulator configurations, underutilizing the loading criteria on the tower, results in the life extension of the tower.

The electrical components are designed with a lower redundancy factor attributed to mainly compact design and cost savings. Although ACSR conductor design have not significantly changed in the 50 years since its inception, there is a growing need to understand its behavioural properties, especially its ageing mechanism [9]. Similarly, silicone composite longrod insulators have had a 30-year evolution in terms of materials utilized to replicate and replace the robust glass insulators. The use of composite materials proves challenging, with each material incorporated, additional degeneration properties emerge in the composite material. The effect of the mechanical and electrical stress placed on the insulator requires, understanding for both the immediate and ageing related failures. It is a well-documented observation that coastal environments alter the insulation properties of the insulator's hydrophobicity, however the overall ageing of the insulator surface is not fully understood and warrants further investigation [10].

2.2 Asset Management Principles

Effective asset management principles utilise efficient systems and resources to monitor, analyse and implement corrective measures ensuring that the assets economic life is capitalize on [11]. However, for these interventions to be executed, the asset useable lifespan needs to be determined on the onset of the asset installation. This may be achieved by utilizing models that predict the economic life of the asset or risk models that prescribe that the asset be renewed after a certain period based on impact of failure, nevertheless benchmarks are required for an effective strategy execution. The ageing characteristics or end of life probability can be estimated with several techniques; however, the most common plot is the Weibull Probability Distribution [12]. The result of the Weibull probability distribution is shown in figure 2-1 [13],

where the component undergoes three stages in the lifespan and the resultant shape of the probability plot is represented by the shape of a “basin curve”.

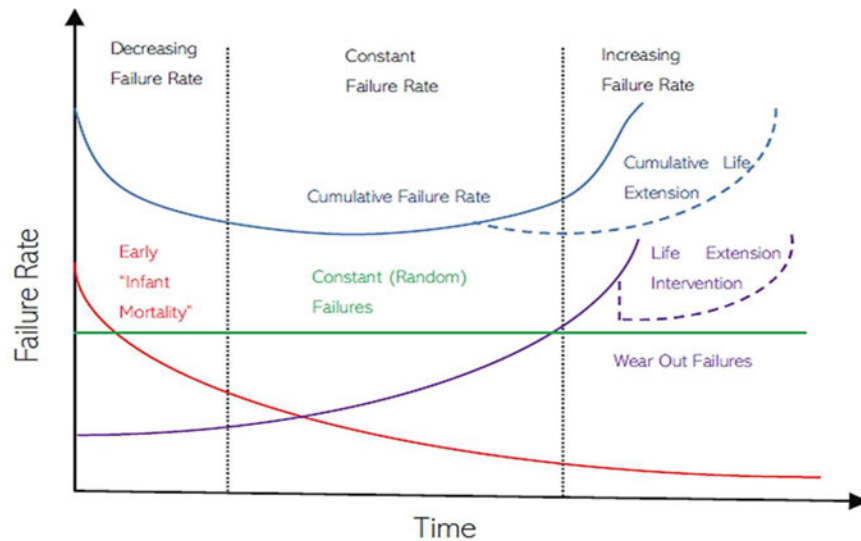


Figure 2-1 Basin curve representing the failure rate of equipment

Understanding the stages of the “basin” plot aids in understanding failure types, allowing asset manager to rest assured that the failures experienced within a component’s lifecycle, are acceptable. These failures can be explained graphically into three main regions namely [14, 15].

Infant Mortality – These failures are generally experienced in the first generation of a component design and installation, where designs may require adapting to suit in-situ conditions in some cases, the component may not be suited to the environment to the extent that infant mortality failures remain high through the asset lifecycle. An example of this is the earlier evolution of silicone composite insulator. Cycloaliphatic insulators were utilized with poor results until it was removed for high voltage applications. Other examples of high infant mortality may be attributed to manufacturing, material, or installation deficits.

Normal life – The failures decrease from the higher infant mortality rates and is demarcated by a lower stabilized failure rate. The failures experienced within this period relate to the stress that the component is exposed to, as well as the performance of the materials utilized its construction. Random failures are experienced, with minimal performance impact. Asset managers seek to maximise the period in this section of the graph, which is the definition of a component’s useful lifespan.

End of Life – The failures experienced at the component end of life stage, is evident by the increasing rate of failures. This may be attributed effects of stresses that results in material degeneration and/or ageing of the component in its entirety (mechanical, electrical, chemical, or thermal). As the failure rates inclines, the

asset manager should evaluate the impact of the failures and determine a course of action to curtail the failures or run the component to failure. Depending on the outcome of the assessment, refurbishment or replacement may be chosen as a life extension intervention [14].

British Standard- PAS 55 has been adopted and provides the framework for ISO 55000 in the South African power utility environment, providing the guiding path in the asset management strategy. The strategy assists utilities, service providers and manufacturers to establish the benchmark minimum performances, for their service or product. Table 2-1, guided by NRS-093-1 [16] provides the minimum lifespans expected from electrical systems and components in an electricity distribution environment. The minimum prescribed useful life for High Voltage lines are requires challenging as this is based on the economic life of the asset and not the technical life. Research into the asset lifespan ranges, for each asset classes, will assist in adequately planning for life extension interventions.

Table 2-1 Prescribed minimum lifespan of electrical equipment according to NRS 093-1

| Asset class | Expected useful life (years) |
|---|-------------------------------------|
| HV transformers | 50 |
| HV lines | 50 |
| HV cables | 50 |
| HV substation equipment | 50 |
| MV transformers (transformers and mini-substations) | 45 |
| MV cables and lines | 50 |
| MV substations switchgear | 45 |
| LV network (overhead) | 45 ^a |
| Network management | 20 |
| Consumer electricity meters (credit type) | 30 ^b |
| Telemetry | 20 |
| ^a Sixty years, if underground cables. | |
| ^b Ten years, if pre-paid meters. | |

2.3 Insulator Ageing

The increased reliability, compactness and cost-effective requirements being placed on insulator designs and manufacturing, has warranted the research into alternative insulator materials. Porcelain insulators were introduced as an insulating medium in the 19th century [17] leading on to glass cap and pin insulators. Porcelain insulators, still prove to be a viable alternative at lower voltages, in the form of post insulators, due to porcelain’s excellent moldability in manufacturing and compressive strength. Glass insulation evolved from the porcelain post insulators into “bell” shaped cap and pin insulator discs that could be coupled to form any insulating length. It was simple in design and construction, robust in installation and possessed excellent self-healing properties. Most importantly, surface tracking and flashovers were visible during failures, however its size, weight, and poor performance in contaminated environments, paved the road for a new type of insulation called Non-Ceramic Insulators (NCI). The majority of glass insulation

failures are attributed to the mechanical failure of the cap and pin owing to corrosion in high contamination environments resulting in the use of polymer insulators [18].

Although shed profile design differed from manufacturer to manufacturer, the silicone composite insulator utilized common designs, consisting of silicone rubber sheds on a semi-flexible, glass fibre loadbearing core [19]. The main function of the silicone rubber is to provide an insulating medium from the environmental effects of heat, humidity, and chemical attacks, but most importantly to provide electrical insulation in the form of a high resistance path, from the live and dead-end components. Composite insulators are mainly utilized at sub transmission and transmission voltages, manufactured to the specified creepage length. Globally, first generation composite insulators have been installed since the 1960's, however ageing and performance vary according to the climatic conditions, making lifespan predictions challenging [20].

2.3.1 Insulator Properties

The hydrophobic surface is attributed mainly to silicone's ability to repel water, providing a uniform protective sheet over the core and similarly provide a high resistive insulating medium. The two leading sheet polymer technologies are ethylene propylene diene monomer (EPDM), which has a higher resistance to tracking related faults and silicone. While the EPDM has higher mechanical strength, silicone composite has a significantly higher resistance to ultraviolet radiation and better hydrophobic properties, under high contamination conditions [21]. Silicone composite insulators are composed of three distinct parts namely the core, the housing, and the end fittings. The core is comprised of mainly glass fibres entrenched in a resin capsule. Electrical (E) or Electrical\ Chemical (E-CR) glass fibres are used in the construction of the core, providing resistance to acid attacks. The saturating resin, a strain of Bisphenol A (BPA) epoxy, provides strength with a small degree of flexibility. Other coatings exist such as ethylene propylene diene monomer (EPDM), ethylene vinyl acetate (EVA), and epoxy resin such as cycloaliphatic, etc. however for the purpose of the study, these coatings will not be explored.

The clamping or attachment-end of the insulator is provided by ends fittings, which houses the glass fibre rod shown in figure 2-2. End fittings, usually made from cast iron, steel or aluminium provide the mechanical strength from handling damage. The section of the insulator between the two metallic end fittings along the profile of the sheds, is known as the creepage distance.

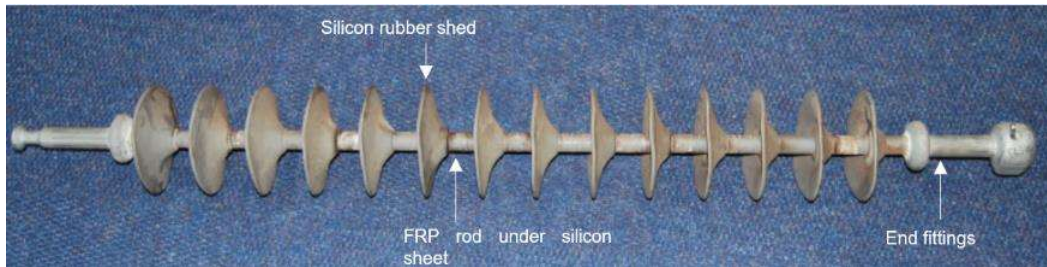


Figure 2-2 Structure of a composite insulator

The housing is composed of silicone rubber (polydimethylsiloxane, PDMS) which is the most common insulator coating. The silicone oxygen (Si-O) bonds are strengthened by the addition of base compounds from the methyl (CH₃), the vinyl and phenyl groups. These combinations are cured in a process of High Temperature Vulcanising (HTV) or at Room Temperature Vulcanising (RTV 1 or 2) or may remain in a liquid state known as Liquid Silicone Rubbers (LSR). The silicone rubber provides an insulating layer for the outer surface of the insulator, however, the layer between the fibre core and silicone rubber, is occupied by a filler material. Filler agent commonly utilised is Alumina Trihydrate (ATH) with the addition of plasticisers and colouring agents. The sheds are added to provide sufficient creepage distance, thereby allowing the insulator to become more compact over glass. Silicone rubbers ability to resist uniform wetting is known as hydrophobicity, which is a dynamic property, repelling leakage current flow under normal service conditions, changing to hydrophilic under stressed or fault conditions [22]. However, once the stress or fault conditions are removed, the hydrophobic layer may be deformed by the energy released during the fault, render the insulator unable to withstand the nominal operating voltage.

The ATH fillers tend to migrate to the insulator surface, reacting with acidic compounds found in high contamination environments. The resultant solution is hydroxyl-based compounds that are transformed to water, further protecting the hydrophobic layer. Unfortunately, the consistent migration of ATH to the insulator surface, has an unlimited lifespan. The voids left by the migration becomes evident in by the creation of micro pores, cracks, and crevices [23].

Insulators, either glass, porcelain or silicone composite suffer from similar types of stress related failures. These stresses are avoidable in terms of system requirements in certain cases while other circumstances, they occur naturally. The dominant stress mechanisms that affect the lifespan of an insulator are as follows, namely:

- Temporary switching, usually from the closing of a breaker or loading and unloading of a line.

- Lightning strikes in the form of direct and indirect strikes on the phase conductor or shield wire resulting in a back-flashover.
- Power frequency contamination flashover.

The primary source of switching transients is created in response to fault interruption by the opening of a breaker at 88kV or 132kV. The switching overvoltage's produced as a result of the arc restriking is between 2% and 13% at a sub transmission level [24]. However, the system including the breaker design is rated for 110kV and 145kV for an 88kV and 132kV system respectively. Transient temporary overvoltage's within a sub transmission system are generated from the switching in or out of components such as capacitor banks and series reactors [25]. The overvoltage is limited by effective system modelling, which recommends smaller banks of capacitors to allow incremental increase in reactive power. Other sources of switching transients include the opening of an unloaded capacitive or inductive line which can result in a transient overvoltage [26]. If the switching overvoltage's cannot be avoided, the effects of the transients can be minimized to within acceptable standards by the installation of surge arresters on sub transmission lines and series or parallel compensation and closing resistors within the substations [27]. Modern distribution systems are designed in accordance with IEC 60071-2 [28] with regards to insulation coordination therefore the impact of transient faults on insulation are minimized and will not be investigated further. Other forms of transient overvoltages are experienced by natural phenomena namely, lightning. Therefore, switching overvoltage's are accommodated within the breaker design specification, excluding this state from the study area.

Lightning activity either sourced from a direct or indirect strike, travels via the shield wire or tower in search for natural ground. If high impedance path is encountered, the resulting surge current attenuates up towards the phase conductor bridging the insulator air gap (back-flashover). The surge impedance of the tower and the parallel surge impedance of the shield wire to which is bonded to the tower, confines the high voltage impulse. The line and tower impedance coupled is not significant enough to dissipate or reduce the overvoltage to within safe limits; therefore, the fault is required to safely conduct to ground via the tower and the low resistance path to earth i.e., the tower foundation. There are several factors that contribute to the managing of the overvoltage, the first being the presence of tower surge arrestors, which may dissipate the overvoltage if placed correctly. The second is the geometry and its effect on coupling between the shield wire and phase conductors. The third is the tower footing resistance or the low impedance conductive path from the tower to the ground. These mitigations have been incorporated into line design to motivate against lightning faults. Additionally, the lightning flash density maps show low lightning activity in coastal areas [29], therefore the effects of lightning will be excluded from the study area.

2.3.2 Contamination Flashover

Contamination flashovers occur as a result of the flow of a leakage current on the insulator surface, leakage current being the current that flows from the live conductor to any point of ground, via the outside surface of the insulator [33]. Silicone rubber provides a highly resistive surface to oppose the flow of current, but contaminants temporarily alter the strength of the resistive layer. As a self-restoring mechanism, silicon has the ability to temporarily incorporate the contaminants into the resistive layer of the insulator surface retarding the flow of a leakage current. However, the cyclic contamination deposits, cleaning, by rain and wind abrasion, results in the diminished capacity of the silicone layer [30-32].

Ultimately, leakage current is influenced by several factors, contamination and wetting being the most significant. The influence of additional parameters, such as, leakage-path length, contamination uniformity and profile on insulator, affect the magnitude of the flashover voltage. However, for the insulator lifespan prediction these will be assumed to be fixed parameters. The four main conditions that need to be met for contamination flashovers to occur at rated working voltage are surface contaminants, humidity, temperature, and altitude.

2.3.2.1 Temperature

The degeneration of the insulation during a flashover is dependent on the maximum temperature transferred to the silicone material and the duration of the applied fault. The composite insulator the glass fibre rod core, which is composed of either polyester, vinyl ester or epoxy resin, epoxy resins, possesses superior thermal stability up to 400°C [34]. Silicone rubber, however, is only stable up to a maximum temperature of 250°C, rendering it the weakest part of the insulator. ATH is used as filler material mainly attributed to its temperature stabilization abilities as well as its ability to neutralize the effects of acidic compounds found in contamination layer. Maximizing the use of ATH would be beneficial to the constitution of an insulator, however an excess of ATH will result in compromised sheet tensile strength resulting in excess elongation of the insulating layer. The energy released in a flashover is sufficient to damage an insulator along the arc-path, severely damaging the insulator and rendering it unusable [35].

The temperature related to high contamination coastal environments, is relevant to ambient temperature under which the insulator operates within. IEC 60815-1 [36] prescribes 20°C as the activation energy required for contamination solution to take effect., The solution conductance varies of temperatures below 20°C is much lower than that above 20°C [37,38]. Additionally, under normal operating conditions, the ambient temperature influences hydrophobicity recovery when wet. An increase in ambient temperature allows for the evaporation of droplets of the insulator surface, increase the dry bands between droplets resulting in an increase in flashover voltage [39].

2.3.2.2 Rainfall and Humidity

Silicone composite insulators, as with all equipment and components, strive to be environmentally friendly in their operating lifespan, by limiting the leached of toxic substances from the insulator surface [39]. As the insulator ages, the ATH migrates to the insulator surface and may be washed into the environment in high humidity and rainfall areas. Legally, compounds utilised in the insulator structure, should have a low porosity value enabling it to be applied to a range of environmental, geographical, seasonal, and climatic conditions [40].

Rainfall contributes significantly to clearing the contamination layer that resides on the insulator surface thereby alleviating the stress build-up by the soluble material deposits. However, over a lengthy period, the washing process erodes the insulator hydrophobic layer by the abrasive cleaning action that is initiated by insoluble contaminants [41]. The amount of wetting in co-ordination with the contaminant on the insulator surface, determines the rate of conductance [42]. The wash off model assumes that after each event, where a threshold rainfall of 10mm/min is reached, the intensity of the rain is sufficient to clear the contamination layer. The Equivalent Salt Deposition Density (ESDD) layer decreases with the higher rain intensity. Figure 2-3 shows that conductivity may start from 1.5mm/min rain and could reach conductivity values of 1000 $\mu\text{S}/\text{cm}$ at a 10mm/min in storm conditions. [43, 44].

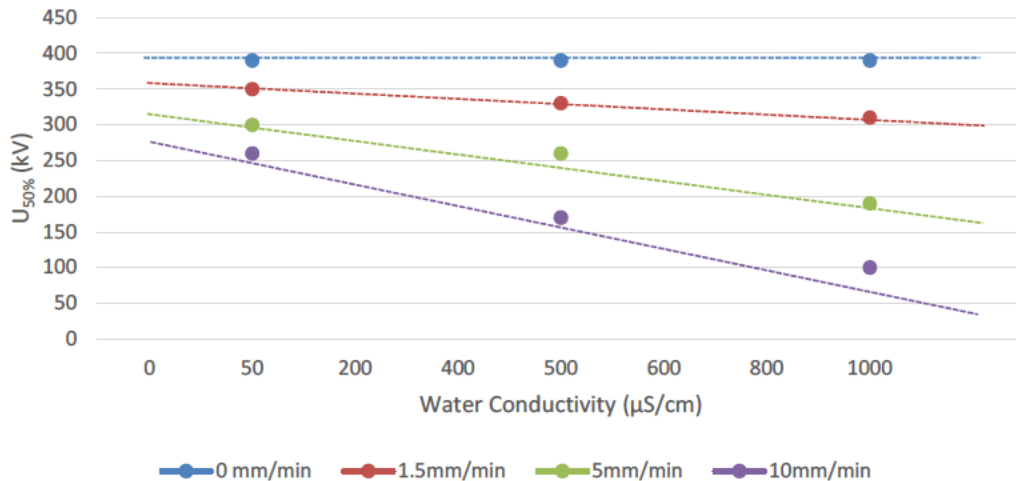


Figure 2-3 $U_{50\%}$ Voltage for 132kV insulator with varying rain flow rates in an E5 contamination environment

2.3.2.3 Insulator Surface Contaminants

The chloride deposits from the coastline (0-5km from sea), are deposited on the insulator surface in a solution state [15]. The “salt mist” traverses up to 5km inline, without any additional form of wetting, to

form a conductive saline solution. A measure of the salt deposits on the insulator surface or equivalent salt deposition density (ESDD) can be calculated using equation 2.1 where the soluble deposit defines ESDD over the insulator surface.

$$ESDD = \frac{M_T \cdot Q}{A} \quad \dots (2.1)$$

M_T is the salinity (mg/cm³)
Q denotes the distilled water (cm³)
A represents the area of the insulator surface

The solution conductivity, which is governed by IEC 60815-1, provides an indicative value of saline deposits in the various contamination categories. These values can be extrapolated to reveal the minimum and maximum solution conductivity values, using $S_a = (5.7\sigma_{20})^{1.03}$ where S_a is the salinity deposit at 20°C (table 2.2) [45-47].

Table 2-2 Various site severity classes based on ESDD and DDDG measurements in South Africa (2001-2005) and IEC 60815-1

| ESDD (mg/cm ²) | NDSS (mg/cm ²) | Site Contamination Severity | Distance from Contamination Source (km) | | Solution Conductivity σ (μ S/cm) | |
|-------------------------------|-------------------------------|-----------------------------------|---|-----|---|-----|
| | | | Min | Max | Min | Max |
| 0-0.01 | 0-0.015 | Very Light (E1) | >50 | | 0.0 | 3 |
| 0.01-0.03 | 0.03-0.06 | Light (E2) | >10 | 50 | 3.1 | 6 |
| 0.03-0.06 | 0.10-0.20 | Medium (E3) | >4 | 10 | 6.1 | 12 |
| 0.06-0.10 | 0.30-0.60 | Heavy (E5) | >1 | 4 | 12.1 | 24 |
| >0.1 | >0.8 | Very Heavy (E7) | 0 | 1 | 24.1 | 50 |

Contamination deposits on polymer insulators alter the surface tension in a two-stage process [48]. Initially, the contamination layer temporarily bonds to the hydrophobic insulator surface, allowing the silicone rubber to gradually incorporate the contamination layer into the insulator protective layer. Wetting has an effect of removing the temporary layer of deposits if heavy wetting is experienced. Light wetting, however, provides the conditions for lowering the surface resistivity of the insulator surface. The second effect of the contamination deposits is one of the insulator surface abrasions [49]. The rate of material degeneration is dependent on the velocity of the wind, the wind direction, and the distance from the particle source [50]. The result of the process is the gradually abrasion of the insulator surface, leading to microscopic crevices and cracks. These cracks are cyclically filled with contaminants until the surface resistance of the insulator is compromised, allowing partial discharge and eventually a flashover [51-53].

2.3.2.4 Altitude

The flashover process is dependent on several factors, one of them being the strength of the dielectric air gap. Air gap strength is determined by the air density, which varies with a change in altitude. According to Zhang et al. [54], the flashover voltage of a contaminated insulator will increase as the air pressure decreases; correlating that higher creepage distances are required for higher altitude applications. The altitude correction factor is given by equation 2.2 which is used to compensate for decrease in the withstand strength of the air dielectric medium [55, 56].

$$k_a = e^{m \frac{H-1000}{8150}} \dots (2.2)$$

*m=1 for an ac gap length of shorter than 2m, greater than 2m m=0.6
k_a= altitude correction factor*

According to IEC 60664-1 a correction factor needs to be applied for every 1000m gained in altitude to account for the reduced air densities. Considering that the altitude is at a minimum in the coastal environments, the correction factor will not be utilized in the study.

Table 2-3 Changes in Air Pressure & Relative Density with Altitude

| Altitude | Sea Level | 1000 m | 2000 m | 3000 m |
|-------------------------------------|-----------|--------|--------|--------|
| Average Air Pressure (MPa) | 0.1013 | 0.0897 | 0.0794 | 0.0704 |
| Ave. Air Pressure (mmHg*) | 760 | 673 | 596 | 528 |
| Average Relative Air Density | 1.0 | 0.901 | 0.812 | 0.732 |

*1 mmHg = 133.3224 Pa

2.3.2.5 Probability of Flashover

The risk of flashover as per IEC 60815-1, is given by the contamination stress probability function $f(\gamma)$, probability of flashover at operating voltage and cumulative distribution function $P(\gamma)$. Multiplying $f(\gamma)$ and $P(\gamma)$ results in the area under this curve, which defines the flashover risk region. The flashover region highlighted in Figure 2-4 is achieved by varying the voltage, contaminants, wetting and temperature on the insulator surface until a flashover is achieved. The minimum flashover voltage at fifty percent of the wet flashover rating is represented as $U_{50\%}$. However, in normal operating conditions the voltage is fixed, and the variables are wetting, temperature and contaminants especially in a coastal environment. Ultimately, the probability of flashover can be represented by the power triangle where, for a leakage current to flow across the insulator surface, with a fixed operating voltage, the resistance values of the insulator surface if

found to be the variable. The loss of surface resistance over a period will result in a flashover at normal operating voltage.

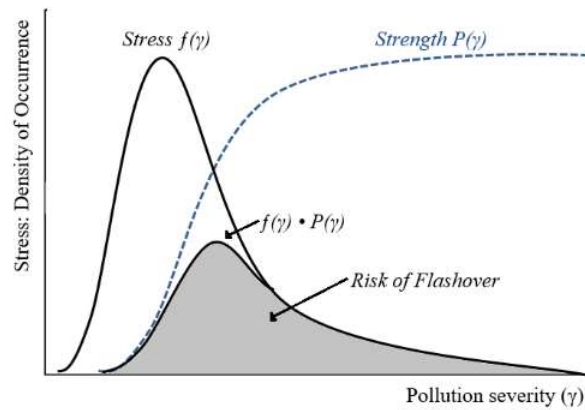


Figure 2-4 Probability distribution function showing the risk of flashover[36]

2.4 Phase Conductor and Shield wire Ageing

The economical evaluation of new line design and construction is dependent on various factors, the most important being the amount of power transferred. Conductor selection satisfies immediate load requirements as well as future growth, within reliability, operability, and safety parameters. The evolution of conductor materials allows for a choice of conductor types, each differing by tensioning strength, conductor diameter, combinations of strength and conductivity and so on. Unfortunately, utilities require the standardization of conductor types for availability of spares, bulk purchasing savings, in-situ applications, environmental requirements and to match the existing tower infrastructure-loading capability [56].

The sub transmission grid is constituted of a wide variety of types e.g., Aluminium Conductor Steel Reinforced (ACSR), All Aluminium Alloy Conductors (AAAC), Hot-dipped Galvanised Steel Wire and to a lesser extent All Aluminium Conductors (AAC). Each type of conductor series serves a specific function wither of current carrying capability, tensile strength or merely for mechanical support. Historically, ACSR was used extensively as an alternate to copper conductor, however, as ACSR aged, applications in coastal regions showed a higher rate of degeneration than inland applications, warranting the use of AAAC conductor in high corrosion applications [18].

2.4.1 Properties of Phase Conductor and Galvanized Steel Shield wire

Common installed ACSR phase conductors have provided economical, high tensile strength and good conductive properties which has warranted its use on most environments. The applicability to corrosive environments, such as the coastline (chlorides), agricultural crops (nitrates) or industry (sulphates) have been placed under scrutiny. Recently, AAAC has proven to be an excellent alternative with better corrosion resistance properties, however, at a higher cost, therefore that application is mainly limited to high corrosion environments.

ACSR conductor, usually the four or five layered (figure 2-5), offers adequate mechanical strength and corrosion resistance, with the two outer or three outer layers providing the electrical conductivity properties [57] while the two or three inner layers provide the mechanical strength. The added advantage of a multi-layered configuration is the aluminium layers protect the galvanised steel cores from corroding with the aid of conductor grease.

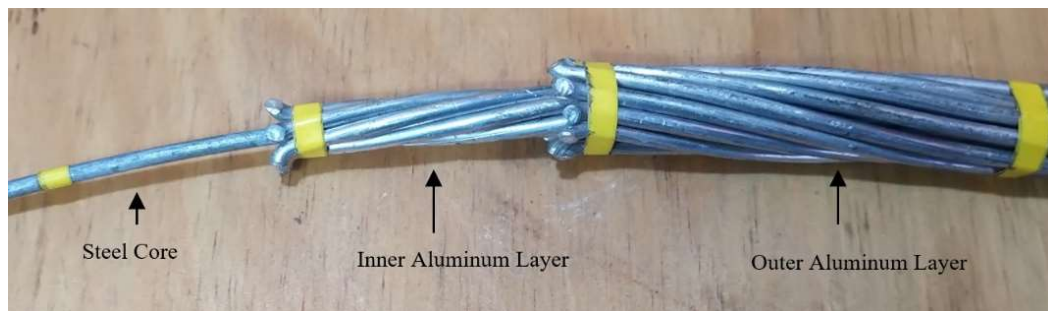


Figure 2-5 Cross Sectional view of a 4-layer ACSR conductor

The type of aluminium alloy utilized in the composition of the ACSR conductor is AA 1350-H19, which is selected for properties of high strength, low ductility, and the higher level of aluminium purity [58]. The aluminium has increased conductivity over standard aluminium and the increase in electrical properties are 62% of that of copper [59]. Additionally, the AA 1350 aluminium offers a higher corrosion resistance and higher weldability as compared to the aluminium series of alloys. Figure 2-6 provides an indication of the properties of a 1350-H19 aluminium, where an exponential relationship exists between strand diameter and tensile strength [60]

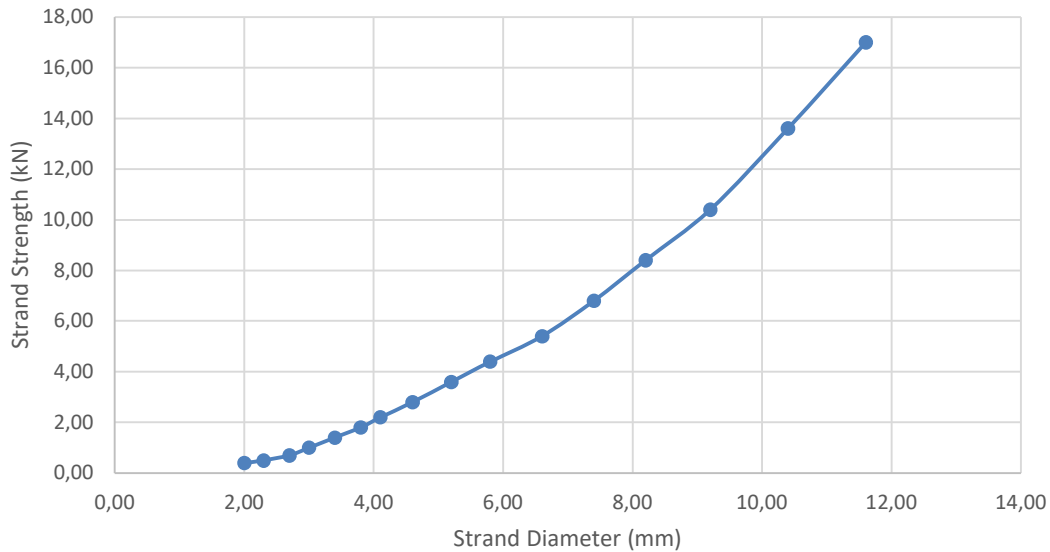


Figure 2-6 Aluminium strand strength (1350-H19) utilised for ACSR conductor

ACSR inner steel core is comprised of either a single or a double layer galvanised steel wire. In most occurrences, the steel strand diameter is the same diameter as the aluminium strands, to ensure that the spaces between the strands are reduced. Class A galvanised steel wire (figure 2-7) [61] is utilized as the structural steel in ACSR, with the different strand diameters and the associated strengths. There is a linear relationship between the diameter and tensile strength of the steel strands.

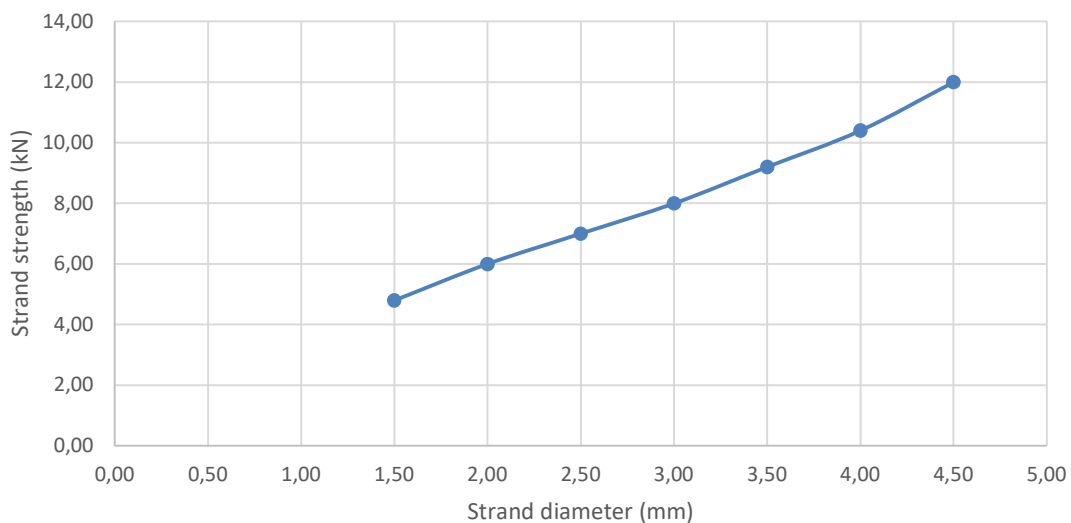


Figure 2-7 Galvanised Steel wire strand strength for Class A galvanised Steel wire

2.4.2 Corrosion Types

Conductor degeneration through environmental ageing mechanisms, vary on the ambient conditions that the conductor is exposed to. AAAC, AAC and HTLS conductor have inherent design mitigation against the effects of environmental degeneration, which ensures a longer technical life of the conductor. ACSR conductor, however, is affected by mechanical stresses, which is indirectly related to corrosion. The side effects of the stress are the loss of conductor material which results in decrease of conductor tensile strength.

The electrochemical process involves the removal of Iron (Fe) removed from the steel core of the conductor via a conductive solution. The solution has dissolved hydroxides that contribute to the formation of rust which is a bi-product of the corrosion reaction. There are various types of corrosion that may affect the conductor, but three main types are prominent in coastal corrosion namely pitting, galvanic and atmospheric [62].

2.4.2.1 Atmospheric Corrosion

Atmospheric corrosion is the most common type of corrosion involving the gradual degeneration of a metal by the oxidation in co-ordination with the contaminants contained in air. The electrochemical process takes place in a high precipitation environment where a soluble solution is created with the contaminant (concentration of sulphates, nitrates, and chlorides deposits on the substrate) [63]. When the solution encounters a metallic substrate, an electrolytic process is established resulting in erosion of the sacrificial material. Steel shield wire and the inner steel core of ACSR phase conductor are subjected to this type of corrosion, however, the aluminium once oxidized, produces a film over the aluminium strands retarding the corrosion process in such as in ACSR conductor. The rate of atmospheric corrosion is dependent on various factors such as climatic conditions (temperature, humidity, shading from sunlight, and contaminants).

2.4.2.2 Galvanic corrosion

Galvanic corrosion occurs in similar conditions to that of atmospheric corrosion; however, the anode and cathodes are of dissimilar metals. The introduction of a leakage current, allows for accelerated electron loss from the anode to the cathode, ultimately resulting in the loss of surface area on the anodic metal. ACSR conductor is susceptible to galvanic corrosion once the insulating layer of grease is lost as a result of natural weathering or high temperatures [64], however this type of corrosion will not form part of the study area due to the conductor reaching 95% tensile strength well before galvanic corrosion occurs.

2.4.2.3 Pitting Corrosion

Pitting corrosion is the second most common form of corrosion seen on most metallic substrates including aluminium and steel. It arises from a concentration of disorganised distribution of soluble chloride, nitrate or sulphate deposits found on metallic substrates. The prolonged contact period between the metal and soluble material results in a release of electrons on the substrate, which is intensified as the “pit” or surface area, grows. If a sacrificial material such as zinc (galvanizing on steel wire) is available, the material is eroded according to the strength of the solution, ultimately resulting in the primary material being exposed to the atmosphere. The depth of pits, which can result in the loss of overall diameter of strand [64]. Pitting corrosion is random and difficult to predict, it occurs at the advanced stages of the corrosion process, therefore it will be excluded from the study area.

2.4.3 Corrosion Ageing

There are several conditions that affect the ageing of conductor such as the wind speed and direction, contaminants, wetting, temperature, etc. Aluminium and steel strands may have corrosion delay mechanism such as aluminium is alloyed and steel is galvanizing, however, these measures delay the inevitable environmental ageing of the conductors. The ageing process is further delayed by the assistance of conductor grease in coastal environments but once the grease loses its protective properties, corrosion takes effect on the conductor [65]. Generally, the grease may still be intact within the inner layers of the multicore conductor, however, the loss of strength on the outer cores due to corrosion is sufficient to cause failure of the conductor. The conditions that contribute the most to the degeneration of the conductor are chlorides, sulphates, and wetness, which dictates the rate of corrosion.

2.4.3.1 Chlorides

In coastal regions, salt or chloride deposits contribute significantly to the corrosion of metallic structures in the form of marine aerosol. The concentration of the aerosol diminished as it traverses inland, wind direction and speed being a contributing factor. The chlorides in co-ordination with the water droplets, provide the molecular weight sufficient to travel short distances in the form of the aerosol. The semi-liquid state of the aerosol prevents crystallization of the chloride molecules thus preventing clumping into large particles with reduced mobility. According to Leeuw et al [66], if the humidity is over 75%, crystallization is prevented.

The consistent aerosol deposits on metallic substrates, aided by the repeated wetting and drying from high humidity environments, raises the concentration of chloride compounds. Consistently, in a humid region, rain follows, washing out the chloride deposits, allowing the process to repeat. Gradually the chloride solution remains sufficiently long enough to initiate the electrochemical reaction of corrosion [67].

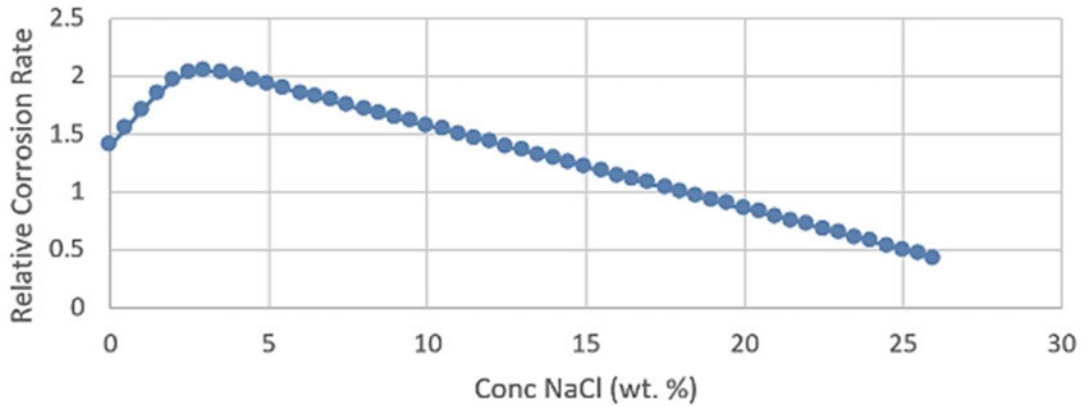


Figure 2-8 Corrosion effect of sodium chloride concentration on iron

According to Hossain [68], chlorine levels vary according to the climatic conditions experienced by the region. These may include factors such as tropical environments, land topography, rise in altitude of the coastline, wind patterns, etc., however, the maximum concentration level is achieved at 3.5% as seen in figure 2-8.

Various authors suggested corrosion rates at various geographic test locations [68-74]. These tests were carried out by the placement of dust gauges at various global points in coastal regions and measurements taken were relative to windspeeds, the ocean salt spray concentration, the topography of the land as well as the climatic conditions experienced. The daily chloride density deposits rates, ranging from 1.2 mgm²/day to 525 mgm²/day, however, the range of 1.2 mgm²/day -23 mgm²/day is most relative to measured values in South Africa (table 2-4).

Table 2-4 Global studies of salt deposition daily rates

| Reference | Marine Environment | Distance from the sea (m) | Salt deposition (mgm ² /day) |
|-----------|------------------------------|---------------------------|---|
| [68] | Atlantic Ocean Cuba | 1-1100 | 19.5 to 525 |
| [69] | Atlantic Ocean Brazil | 10-1100 | 6 to 460 |
| [70] | Indian Ocean | 93-7012 | 1.31 to 54.02 |
| [71] | Atlantic Ocean | 50-13550 | 11.8 to 138.1 |
| [72] | Spain | 300-2500 | 11.6 to 1905.5 |
| [73] | Atlantic Ocean French Guiana | 4000-13000 | 15.7 to 22.4 |
| [74] | South Africa | 1-2000 | 1.2 to 23.69 |

2.4.3.2 Sulphides

Sulphur dioxide is predominantly created as a bi-product of mainly manufacturing, power generation and in the Petro-chemical industry. Additional sources may include mining, the processing of metals and agricultural use [75]. The sulphur dioxide concentrations fluctuate seasonally, peaking in the winter season, where additional fossil fuel is spent for the purposes of domestic heating. Further, veld fires and cane burning are also experienced during these winter months resulting in airborne contaminants that settle on electrical equipment in fine particle form. Under dry atmospheric conditions, sulphur dioxide combines with air to form sulphur trioxide, however under rain or high humidity conditions experienced in coastal environment, sulphur trioxide combines with water to form sulphuric acid [76-78].

Table 2-5 shows the concentration of sulphur dioxide emitted from various sources globally, with the highest concentration attributed to industrial contaminants. Figure 2-9 [3] provides an indicative map of sulphur dioxide concentrations in South Africa, with a 0.05 to 0.1 Dobson (0.0010708 $\mu\text{g}/\text{m}^3$ to 0.0021415 $\mu\text{g}/\text{m}^3$) within the coastal environment.

Table 2-5 Potential sulphur dioxide levels generated from various sources.

| Pollutant | Concentration Deposition (yearly average) | | Source |
|------------------|--|---------------------------------|--|
| SO ₂ | Rural | 2-15 $\mu\text{g}/\text{m}^3$ | Atmospheric/ agricultural |
| | Urban | 5-100 $\mu\text{g}/\text{m}^3$ | Petroleum based combustion |
| | Industrial | 50-400 $\mu\text{g}/\text{m}^3$ | Processing, mining, petroleum combustion |

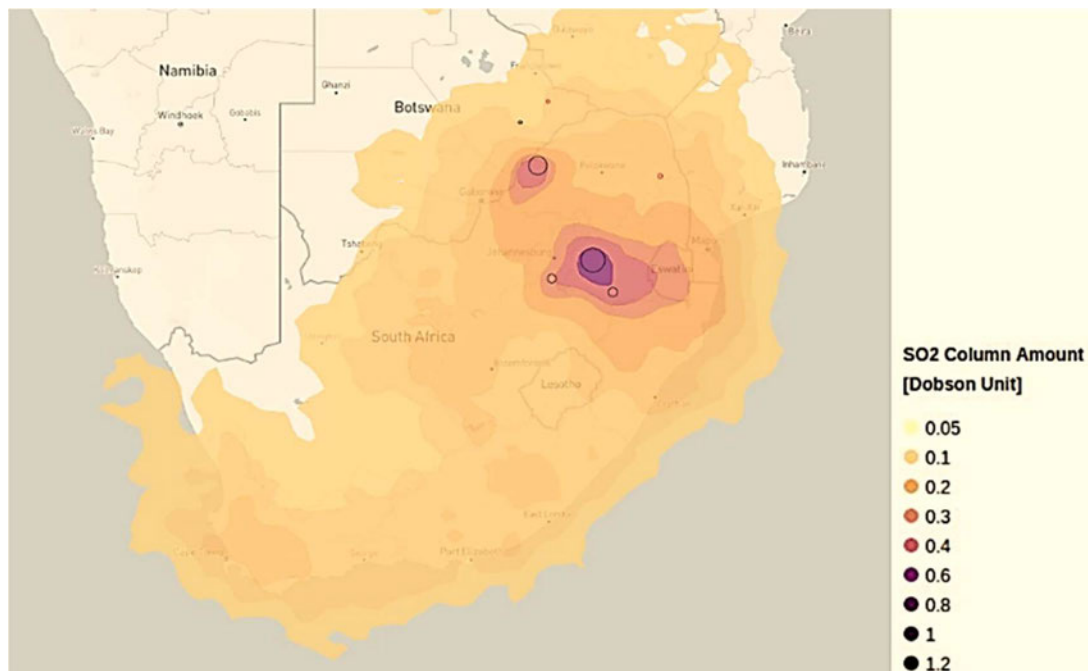


Figure 2-9 Sulphur dioxide concentration map of South Africa [75].

2.4.3.3 Wetness

A key component in corrosion is the level of wetness that the substrate is exposed to. This may vary in the form of immersed, tropical, or humid environments. The film of moisture aids in the development of an electrolytic solution with the existing contaminants on the substrate surface. The anodic and cathodic process is dependent on the time of wetness as the moisture film is not continuous in cases of rain, fog, frost, and temporary wetting forms of precipitation.

According to ISO 9223, wetness is defined as the period where relative humidity exceeds 80% while the ambient temperature exceeds 0°C. Table 2-6 is adapted from ISO 9223 to incorporate the wetness classes relative to a water body namely the coastal sea spray.

Table 2-6 Wetness classification based on time of wetness.

| Wetness Class | Duration (hour) | Total Wet Annually (h/year) | Distance from Water Source (km) |
|----------------------|------------------------|------------------------------------|--|
| T1 | <0.1 | <10 | >100 |
| T2 | 0.1-3 | 10 to 250 | 50 to 00 |
| T3 | 3-30 | 250 to 2600 | 10 to 49 |
| T4 | 30-60 | 2600 to 5200 | 3 to 9 |
| T5 | >60 | >5200 | 1 to 3 |

2.4.4 Corrosion Failure Probability

The process of corrosion modelling is dependent on exposure of environmental contaminants combining with a liquid medium, to create a solution. Corrosion models vary from linear to quadratic functions to predict the ageing effect on a material substrate. The models discussed by Roberge [79], are coherent for different categories of corrosion however, the degree of corrosion is based on the exposed area of the substrate. Larger bare surfaces may follow a liner corrosion model as the protective film created during the corrosion process may not be sufficient to retard the process. Certain substrates may experience variable corrosion rates as crevices created during the initial process, may retard, or accelerate the corrosion process. Figure 2-10 shows the various corrosion loss models, each being influenced by the climatic conditions and the exposure of the substrate involved [80-82].

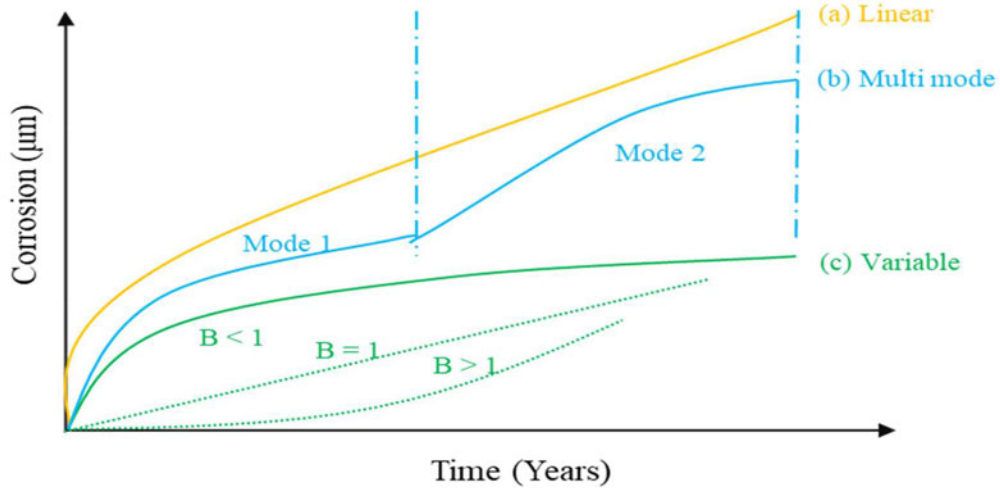


Figure 2-10 Corrosion loss over the material lifespan. (a) Taman (1923) for atmospheric corrosion, (b) Melchers multi-mode corrosion process, (c) Marine and atmospheric corrosion [83]

The model most applicable to the corrosion of steel shield wire and phase conductor is the multi-mode model shown in figure 2-11 [83]. The multimode model incorporates the various stages of corrosion that relates to a multi layered substrate, the three-phase process.

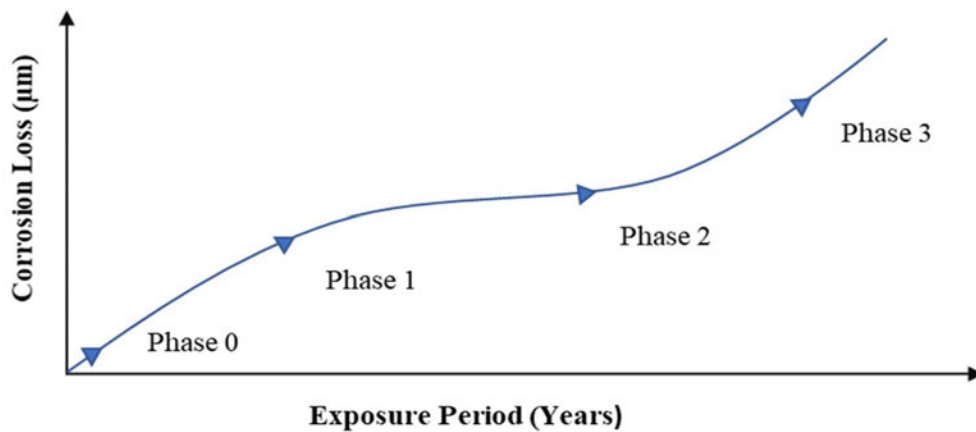


Figure 2-11 Various stages of corrosion in a multi-layered model.

Phase 1 – The movement from phase 0 to phase 1 is encouraged by the contamination medium concentration, the solution concentration and the activation energy released by thermic reaction [84]. This stage occurs within the first few years of the component installation in a contamination environment.

Phase 2 – Once an oxidizing layer is formed on the substrate, the diffusion of solution is retarded by the corrosion product. The corrosion rate remains at a constant over a period until the corrosion product allows the ingress of the contaminant solution. Higher activation energy provided by the higher temperatures, are not sufficient to increase the corrosion rate, as the solution barely penetrates the corrosion product layer [85].

Phase 3 – According Melchers [86], stage 3 denotes the end of the linear rate in corrosion and the initiation of exponential rate of corrosion. This rate continues indefinitely leading to material yield strength failure [63].

2.5 Summary

Sub transmission asset management principles are realised when the useable lifespan of the components is determined and managed accordingly. There are predictive models that provide an indicative economic life of the asset however, to maximise the utilization of the asset, in-situ testing of component degeneration is required. In a sub transmission environment, the components that have the highest failure impact, are the electrical components namely, insulators, conductor, and shield wire.

Silicone polymer composite insulators provide an advantage over other materials due to its hydrophobic surface that is advantageous in superior fault recovery rates. Contamination flashovers are commonly found in coastal regions where the increased leakage current flow on the insulator surface, is attributed to diminished insulator surface resistance. Leakage currents are influenced by several factors, such as, leakage-path length, contamination uniformity and profile on insulator however, for the insulator lifespan prediction model, these will be assumed to be fixed parameters. The four main conditions that significantly contribute to the contamination flashover process are surface contaminants, humidity, temperature, and altitude.

Conductor degeneration as a result of environmental ageing mechanisms, vary on the ambient conditions that the conductor is exposed to. ACSR conductor and galvanised steel shield wire are affected mechanically by the effects of corrosion. The common types of conductor corrosion in coastal environments are pitting, galvanic and atmospheric corrosion with each being dependant on the wind speed and direction, contaminants, wetting, temperature, etc. The model most applicable to the corrosion of steel shield wire and phase conductor is the multi-mode model which incorporates the various stages of corrosion that relates to a multi layered substrate.

CHAPTER 3 MODELLING AND ANALYSIS

3.1 Introduction

Assets management utilize statistical modelling tools for component age modelling, incorporating processes such as failure modes, critical analysis, condition assessment and life prediction analysis. The process involves modelling of specific component failure behaviour by utilizing condition, operational and environmental data to determine an ageing model. Condition assessments and failure mode analysis makes use of sensor data, however if the component or asset is in its infancy life stage, a theoretical prediction model may be suggested based on available data. These prediction models hinge on probability of failure based on material ageing and may incorporate additional condition-based data as the failure modes become apparent [15]. According to Pham [87], the Arrhenius Weibull function may be the most appropriate model to represent material ageing characteristics over a period. Additionally, the power law may also be utilised as an ageing function.

3.2 Insulator Contamination Flashover Modelling

Ageing of insulators are attributed to the weakening of the resistive properties of the insulator surface, which leads to a flashover over time. Factors that inherently contribute to degeneration of the material hydrophobicity in silicone composite insulation, are environmental factors mainly contaminants and high humidity environments. The contamination flashover can be modelled electrically utilizing the Obenaus model [88], which represents an electrical circuit model of the arc propagation along the insulator surface. The resulting voltage gradient is established by the relationship between the arc current and arc voltage. A key variable in the voltage gradient equation, is the insulator resistance represented by R_a . As the contamination is incorporated into the insulator surface layer, the resistance model can be represented by R_p shown in Figure 3-1 [89].

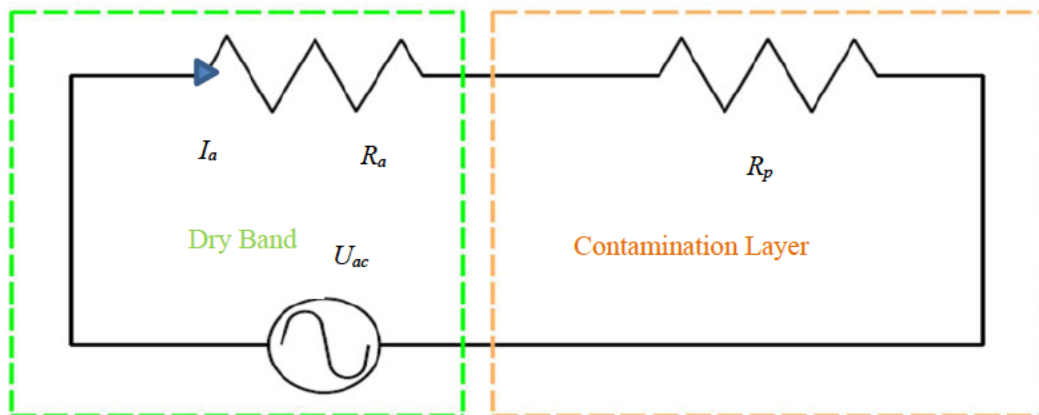


Figure 3-1 Obenaus adapted model of contaminated insulator

Flashovers in high contamination and high humidity environments are influenced mainly by the contamination severity represented by resistance per unit length (R_p) which correlates to the flashover Voltage, applied voltage (V_{fo}) [90-92].

According to Gencoglu et al. [93], the contamination flashover occurs in a dual successive phase. The first is achieved by the temporary reduction in the surface hydrophobicity, encouraged by the contamination layer. The exhibition of miniscule glows or partial discharge at high contaminated solutions points along the insulator shed, highlights the first stage. The reduction of surface resistivity (R_p) which occurs over multiple of contamination and cleaning cycles, results in a consistent glow or discharge over the insulator sheds leading to a flashover.

Rizk [94] and Holtzhausen, [95] proposed an alternative flashover model where, when the surface resistance reaches a critically low value, the insulator will possibly flashover at rated voltage. However, the electrical flashover voltage model proposed by Abdelhalim et al. [55], provides an applicable ageing model, showing the degeneration of the surface resistance over a period. The resulting electrical flashover current can be calculated by equation 3.1 and 3.2 [38].

$$R_p = \frac{L}{\sigma 2\pi r x} \dots (3.1)$$

σ = conductivity of the contamination layer (μS)
 L = creepage path length (mm)
 x = age acceleration factor
 R_p = Ageing resistance value ($M\Omega$)
 V_{fo} = Flashover Voltage (kV)

$$V_{fo} = A^{\frac{n}{n+1}} \cdot R_p^{\frac{1}{n+1}} \dots (3.2)$$

A = Ayrton's arc equation exponent constant (737)
 n = Ayrton's reigniting Constant (0.714)

The form factor of an insulator is an average resistance of the conductive and non-conductive part of an insulator shed. This resistive value is taken as the maximum value before the arc-ignition over the insulator surface [96].

Equation 3.1 provides an estimation of the critical flashover voltage with specific known conditions such as contamination layer and wetting. Additionally, equation 1 assumes that the creepage value remains constant throughout the lifespan of the insulator, which is not the case. The resistivity of the insulator surface is in constant state of fluctuation, influenced by the contamination layer and the gradual erosion of the insulator hydrophobic layer by abrasion. The contamination layer thickness is predicted by IEC 60815-1

which highlights the potential value of ESDD deposits, wind, temperature, particle type in coastal environments.

3.2.1 Accelerated Ageing Factor Insulators

According to Jiang et al. [43, 97] the contamination layer occurs primarily as a result of a seasonal deposit which, is also removed periodically by cyclic rain washing. The manner in which the contaminants are deposited on the insulator surface, affects, or degenerates the surface resistance of the insulator, high speed deposition of contaminants including solid dust or the heavier sand particles by the prevailing winds, abrasively removes a subtle layer of the insulator when deposited and also, when cyclically washed. The surface resistivity values loss is assumed to be exponential as cracks occur on the insulator surface, resulting in high rate of surface resistivity loss. An acceleration factor, to represent the surface resistance degeneration in an E1-E7 contamination environment, is shown in equation 3.3 [98].

$$x = e^m \dots (3.3)$$

x = acceleration factor

m = ratio of predicted to actual performance

The acceleration factor provides a means to compensate for the effect of the predicted and measured failures that are outlined in the asset management philosophy of the component being studied. Rashid [99] provides the data of failure history on coastal sub transmission lines shown in table 3.1, where insulator failures between year 1 to year 13 are identified. The variance between the predicted failures and measured failures are represented by *m* in table 3-1.

Table 3-1 Insulator failure data used to calculate the Ageing Acceleration factor

| Line Name | Insulator Installation Age | Measured Failure Rate (%) | Predicted failure Rate (%) | Difference between Measured and Calculated Failure Rates | <i>m</i> | Average | <i>X</i> |
|--------------------------|----------------------------|---------------------------|----------------------------|--|-------------|-------------|-------------|
| Sub transmission Line 1 | 1 | 1,92 | 1,5 | 0,42 | 0,28000000 | 0,28 | 1,323129812 |
| Sub transmission Line 2 | 2 | 0,25 | 1,5 | -1,25 | -0,83333333 | -0,20000000 | 0,818730753 |
| Sub transmission Line 3 | 2 | 1,13 | 1,5 | -0,37 | -0,24666667 | | |
| Sub transmission Line 4 | 2 | 2,22 | 1,5 | 0,72 | 0,48000000 | | |
| Sub transmission Line 5 | 3 | 0,25 | 3 | -2,75 | -0,91666667 | -0,02800000 | 0,972388367 |
| Sub transmission Line 6 | 3 | 1,41 | 3 | -1,59 | -0,53000000 | | |
| Sub transmission Line 7 | 3 | 0,23 | 3 | -2,77 | -0,92333333 | | |
| Sub transmission Line 8 | 3 | 7,69 | 3 | 4,69 | 1,56333333 | | |
| Sub transmission Line 9 | 3 | 5,00 | 3 | 2,00 | 0,66666667 | | |
| Sub transmission Line 10 | 4 | 0,52 | 3 | -2,48 | -0,82666667 | -0,82666667 | 0,437505209 |
| Sub transmission Line 11 | 5 | 2,80 | 3 | -0,20 | -0,06666667 | -0,26533333 | 0,766950257 |
| Sub transmission Line 12 | 5 | 0,94 | 3 | -2,06 | -0,68666667 | | |
| Sub transmission Line 13 | 5 | 1,54 | 3 | -1,46 | -0,48666667 | | |
| Sub transmission Line 14 | 5 | 1,95 | 3 | -1,05 | -0,35000000 | | |
| Sub transmission Line 15 | 5 | 3,79 | 3 | 0,79 | 0,26333333 | | |
| Sub transmission Line 16 | 6 | 2,89 | 3 | -0,11 | -0,03666667 | -0,27833333 | 0,757044431 |
| Sub transmission Line 17 | 6 | 1,44 | 3 | -1,56 | -0,52000000 | | |
| Sub transmission Line 18 | 7 | 3,31 | 3 | 0,31 | 0,10333333 | 0,10333333 | 1,108860968 |
| Sub transmission Line 19 | 8 | 1,33 | 3 | -1,67 | -0,55666667 | 0,51166667 | 1,668068994 |
| Sub transmission Line 20 | 8 | 7,74 | 3 | 4,74 | 1,58000000 | | |
| Sub transmission Line 21 | 9 | 3,12 | 3 | 0,12 | 0,04000000 | 0,37166667 | 1,450149518 |
| Sub transmission Line 22 | 9 | 5,11 | 3 | 2,11 | 0,70333333 | | |
| Sub transmission Line 23 | 10 | 7,50 | 5 | 2,50 | 0,50000000 | 0,5 | 1,648721271 |
| Sub transmission Line 24 | 11 | 4,55 | 5 | -0,45 | -0,09000000 | 0,416 | 1,515885869 |
| Sub transmission Line 25 | 11 | 1,64 | 5 | -3,36 | -0,67200000 | | |
| Sub transmission Line 26 | 11 | 2,36 | 5 | -2,64 | -0,52800000 | | |
| Sub transmission Line 27 | 11 | 19,77 | 5 | 14,77 | 2,95400000 | | |
| Sub transmission Line 28 | 12 | 6,12 | 5 | 1,12 | 0,22360000 | 0,2236 | 1,250570691 |
| Sub transmission Line 29 | 13 | 5,16 | 5 | 0,16 | 0,03200000 | 0,788 | 2,198994037 |
| Sub transmission Line 30 | 13 | 11,96 | 5 | 6,96 | 1,39200000 | | |
| Sub transmission Line 31 | 13 | 12,04 | 5 | 7,04 | 1,40800000 | | |
| Sub transmission Line 32 | 13 | 9,52 | 5 | 4,52 | 0,90400000 | | |
| Sub transmission Line 33 | 13 | 8,14 | 5 | 3,14 | 0,62800000 | | |
| Sub transmission Line 34 | 13 | 6,82 | 5 | 1,82 | 0,36400000 | | |

By applying equation 3.3, a 13-year acceleration equation represented by $e^{0.0433m}$ is shown in figure 3-2. This equation can be further expanded into the 50-year accelerated degeneration model shown in figure 3-3.

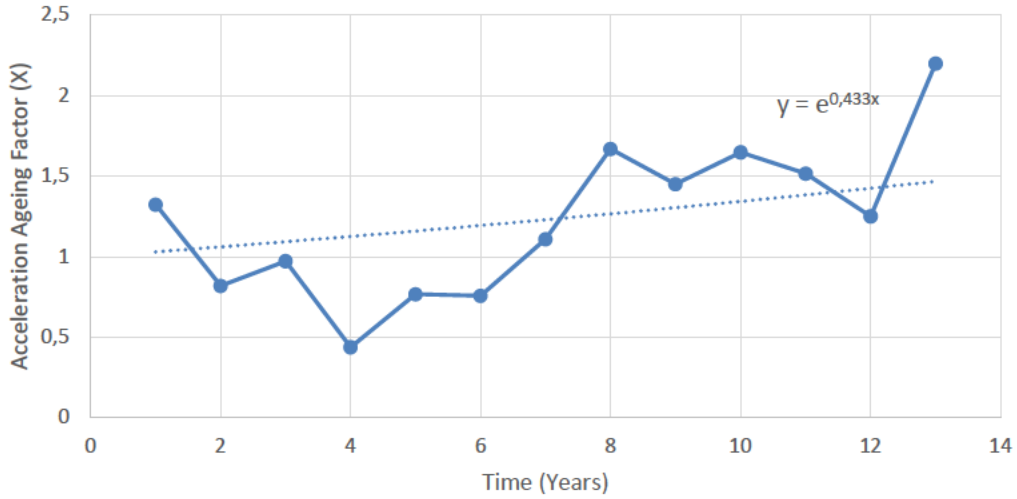


Figure 3-2 Insulator Accelerated Ageing model (13 years)

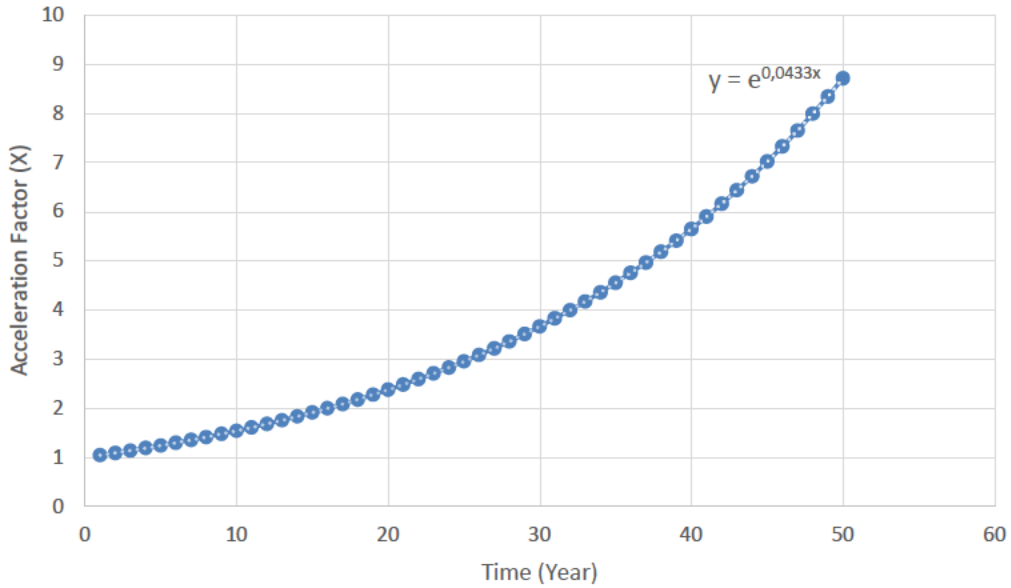


Figure 3-3 Insulator Accelerated Ageing model (50 years)

The probability of temperature related insulator failure given by the Arrhenius life-stress relationship is given by equation 3.4.

$$f(T) = C e^{\frac{E_a}{K.T}} \dots (3.4)$$

C = an estimated parameter

E_a = Activation Energy for polymeric insulation (1.83.44kJ/mol)

R is the universal gas constant ($8.31 \cdot 10^{-3}$ kJ/mol.K)

K = Boltzmann's constant ($8.617385 \cdot 10^{-5}$ eV/k).

The model utilizes the silicone material subatomic properties, with their specific activation energy, to determine a reaction rate. The life prediction model is based on material properties alone, without considering the in-situ conditions that the component is installed in [100].

Applying equation 3.2, the resulting loss of surface resistivity on the insulator surface is shown in figure 3-4 for the contamination categories E1, E2, E3, E5 and E7. The calculation is carried out on a 132kV insulator with a creepage length of 4495mm, shed diameter of 124mm and conductance values from table 2-2, acceleration factor being applied to E1-E7 contamination categories. It should be noted that the main variable in is the conductance values, which are based on averages.

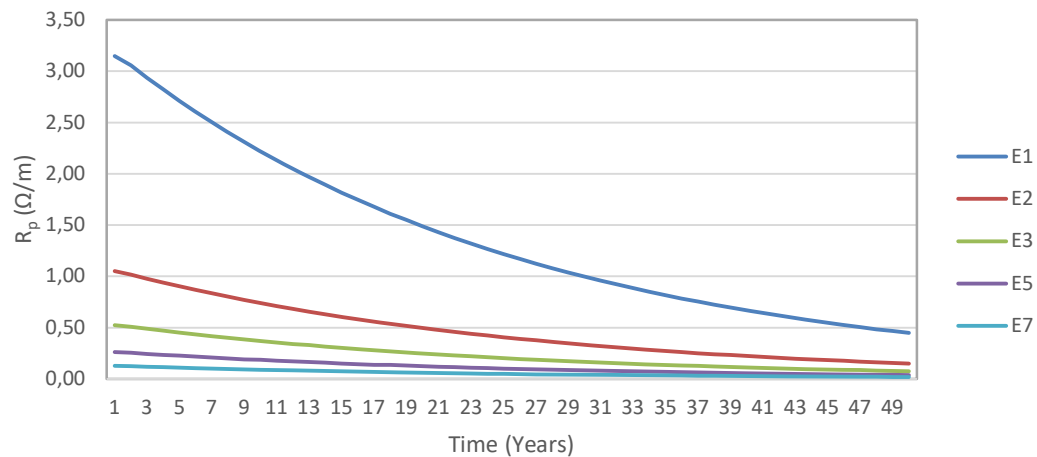


Figure 3-4 Surface resistance degeneration over a period of time

Applying equation 3.3, the resulting flashover voltage profile is shown in figure 3-5 for the 132kV insulator. 31mm/kV, is recommended by IEC 60815 for applications in E5-E7 contamination category, namely coastal environments. However, based on the average conductance values selected, a 132kV insulator is susceptible to a flashover after 7 years and the 31mm/kV insulator is not suitable for a E6-E7 environment mainly attributed to the contamination deposits.

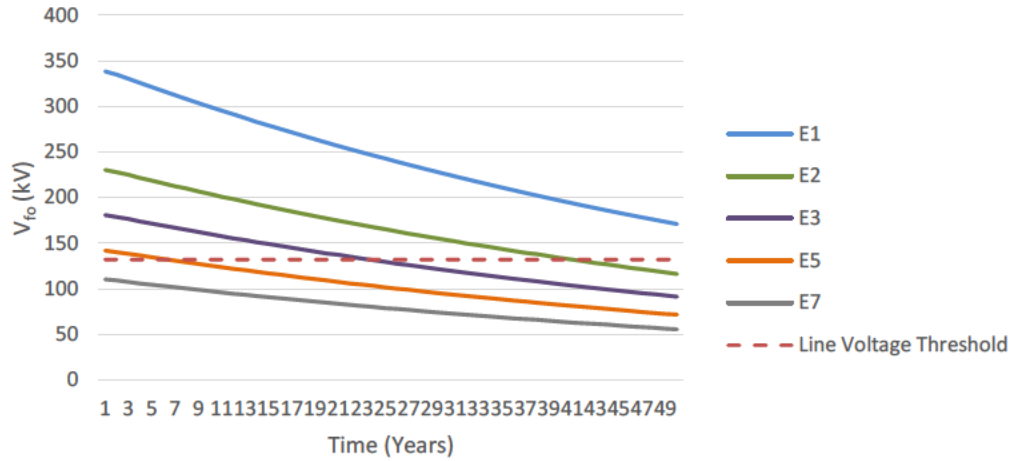


Figure 3-5 Flashover lifespan prediction for 132kV silicone insulator in E1-E7 contamination categories

3.2.2 Insulator Ageing Model Validation

A line was analysed to determine the correlation between flashed insulators, the age of the insulator and the contamination level. The line selected, resided in a E4/E5 contamination category where the minimum distance was 3km, the max being 7km from the contamination source. The line is rated at 132kV and was constructed at an altitude of 200m above sea level. According to Macey [101], the line was reinsulated with composite longrod insulators with the recommended IEC 60815 costal specification of 31mm/kV creepage. The line inspection, which occurred after 15 years, revealed 16 towers of the total 159 towers contained flashed insulators. These positions are listed in table 3-2.

Table 3-2 Flashed insulators and distance from contamination source

| | | | | | | | | | | | | | | | | |
|---|----------------------------------|-----|-----|-----|-----|-----|-----|-----|-----|-----|-----|-----|-----|------|-----|-----|
| Tower Number | 28 | 30 | 32 | 34 | 37 | 40 | 55 | 59 | 61 | 86 | 107 | 116 | 128 | 131 | 147 | 159 |
| Distance from Contamination Source (km) | 9.4 | 8.9 | 8.6 | 8.2 | 8.1 | 7.6 | 4.6 | 4.5 | 4.2 | 4.3 | 3.6 | 3.8 | 5.5 | 6.71 | 6.4 | 7.6 |
| σ_s (μS) | 11.63-21.7 pa, average of 17.811 | | | | | | | | | | | | | | | |

The EDDD values at each site was not available however, data from the source substation was available and reflected annual conductance values of 21.7 μS and 14.3 μS . These conductance values were average out to 17.811 μS which was utilized for the simulation. The insulator attachment height was recorded at 12m to 16m above ground with an average prevailing wind of 4.8km/h and average temperature of 25°C [102]. The line route is shielded by trees, valleys, and industrial building however, at the location of the flashed insulators, the towers generally protrude from the landscape and remain unshielded from offshore winds.

Applying equations 3.2, the result from the analysis is shown in figure 3-6, while the values are shown in table 3-3. There is a correlation between the projected life of the insulators, based on the average conductance values of 17.811 μS within the E4/E5 contamination category, between the measured and projected failures.

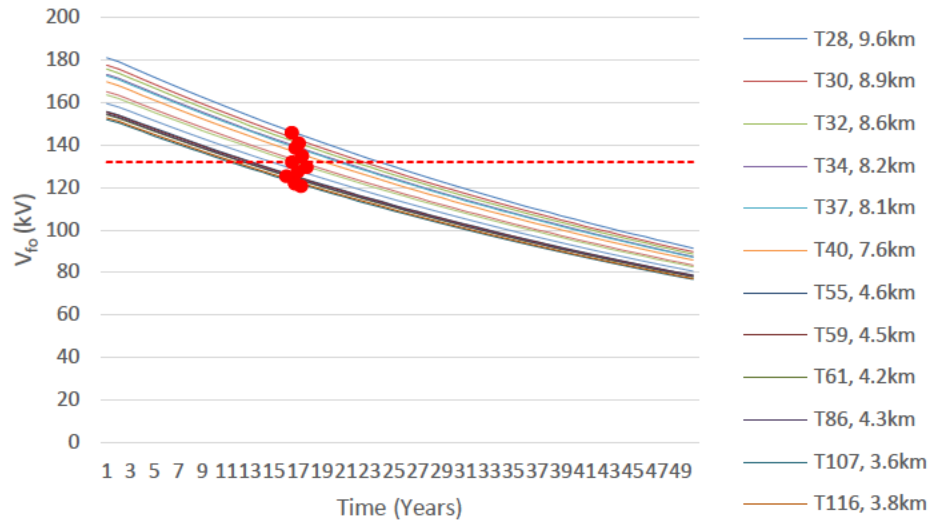


Figure 3-6 Predicted vs Measured insulator failures

The standard deviation plot is shown in figure 3-7 where the average is 2.125 years and standard deviation is 4.286 years. The variance in the measured and calculated values is attributed to the higher ESDD rate on the insulator surface due to specific wind conditions at certain towers. The towers that are closer to the coastline (3-4km) are susceptible to a higher rate of failure, however, the insulators that are further away (up to 10km), have also failed. Based on wind patterns [102] and the topography, there are open channels that allow movement of air directly from the coastline to the towers within the E3 contamination category (10km). This contributes to the higher ESDD values resulting in reduced insulator surface resistance values over the lifespan of the insulator.

Table 3-3 Data for the insulator lifespan variance calculation

| | | | | | | | | | | | | | | | | |
|--------------------------------------|-----|-----|-----|-----|-----|-----|-----|-----|-----|------|------|------|------|------|-----|-----|
| Tower Number | 28 | 30 | 32 | 34 | 37 | 40 | 55 | 59 | 61 | 86 | 107 | 116 | 128 | 131 | 147 | 159 |
| Distance (km) | 9.4 | 8.9 | 8.6 | 8.2 | 8.1 | 7.6 | 4.6 | 4.5 | 4.2 | 4.3 | 3.6 | 3.8 | 5.5 | 6.71 | 6.4 | 7.6 |
| Calculated period for Flashover (kV) | 149 | 147 | 145 | 143 | 142 | 140 | 128 | 128 | 127 | 128 | 125 | 126 | 132 | 136 | 135 | 140 |
| Variance in lifespan (Years) | 8 | 7.5 | 7.5 | 5.5 | 6.5 | 4 | -2 | -2 | -2 | -1.5 | -2.5 | -3.5 | -3.5 | 0 | 2 | 1.5 |

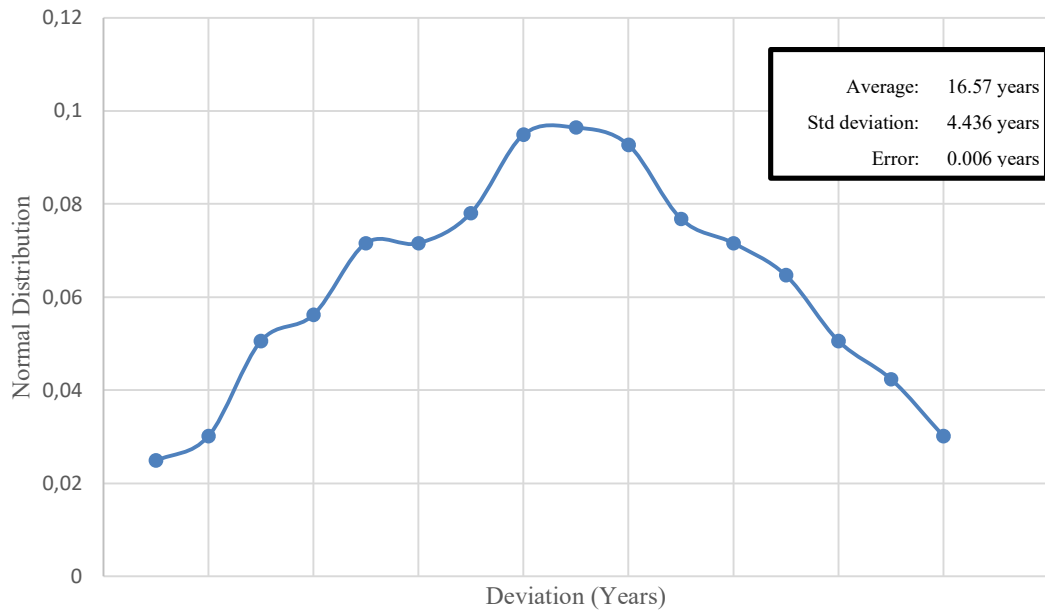


Figure 3-7 The standard deviation for the calculated flashover values

3.3 Conductor and Shield Wire Corrosion Modelling

The primary mode of ACSR ageing failure is attributed to the loss of mechanical strength, of the aluminium and galvanised steel. Aluminium is susceptible to thermal failures in terms of annealing above 93⁰C as well as loss of surface area attributed to corrosion. Thermal fluctuations (sustained faults) during power transfer may result in the premature stressing and failure of the conductor however, aluminium annealing is avoidable during normal power transfer by means of protection circuits. Material corrosion namely, the reduction of strand strength diameter and the resulting loss of strength, is unavoidable and is the main contributor to the ageing process.

Atmospheric corrosion has the most far-reaching effects on material corrosion especially in coastal environments, where humidity and contaminants are largely unavoidable. Corrosion of ACSR conductor occurs in a three-stage process, with some overlaps between stages. The first stage occurs with the corrosion of the outer layers of the multi-layered conductor. The second stage occurs when the conductor grease becomes ineffective resulting in the loss of the galvanizing layer on the steel cores. The third stage is the

corrosion of the steel cores as no forms of protection is offered by the aluminium strands, the conductor grease, or the galvanizing layer. As per SANS 61284 [103], the conductor should be replaced when it deteriorates beyond 95% of the ultimate tensile strength for both shield wire and phase conductor.

Modelling of ACSR conductor is achieved by assessing the effects that corrosion has on Aluminium, Steel and Zinc. ISO 9223 [3] provides a material degeneration rate incorporating environmental conditions such as wetness, sulphur dioxide, chlorides, and temperature. These degeneration rates are represented by equations 3.5 -3.7, however, it is reflective of the first year of corrosion and not the entire lifespan of the material.

ISO 9223 [3] states for Aluminium yearly loss for the first year

$$r_{corr} = 0.0042[SO_2]^{0.73} \exp(0.025RH + f_{Al}) + 0.0018[Cl^-]^{0.60} \exp(0.020RH + 0.094T)$$

$$f_{Al} = 0.009(T - 10) \text{ when } T \leq 10^{\circ}C, \text{ otherwise } - 0.043(T - 10) \dots \text{ (equation 3.5)}$$

SO_2 = Sulphur dioxide (mg/ m².d)
 RH = Relative Humidity (%)
 T = Average Monthly Temperature (°C)
 Cl^- = Chloride (mg/ m².d)

The Zinc loss is represented by equation 3.7 for the galvanising of the shield wire and equation 3.6 for the steel portion of the shield wire.

ISO 9223 [3] states for carbon Steel yearly loss for the first year

$$r_{corr} = 1.77[SO_2]^{0.52} \exp(0.020RH + f_{St}) + 1.02[Cl^-]^{0.62} \exp(0.033RH + 0.040T)$$

$$f_{St} = 0.150(T - 10) \text{ when } T \leq 10^{\circ}C, \text{ otherwise } - 0.054(T - 10) \dots \text{ (Equation 3.6)}$$

ISO 9223 [3] states for Zinc yearly loss for the first year

$$r_{corr} = 0.0129[SO_2]^{0.44} \exp(0.046RH + f_{Zn}) + 0.0175[Cl^-]^{0.57} \exp(0.008RH + 0.085T)$$

$$f_{Zn} = 0.038(T - 10) \text{ when } T \leq 10^{\circ}C, \text{ otherwise } - 0.071(T - 10) \dots \text{ (equation 3.7)}$$

3.3.1 Accelerated Ageing Factor Conductor and Shield wire

Dong et al. [100], suggests that the conductor ageing model should include a fitting or accelerated ageing factor that incorporates the material degeneration profile described in the asset management policies. The Weibull two parameter probability function serves as a generic material degeneration model, however, the power law suggested by Ricker [104] and Melchers [105], shown in equation 3.8, is suited to metal degeneration.

$$y = at^n \dots (\text{equation 3.8})$$

y = acceleration factor

t = time

n = ratio of predicted to actual performance

a = constant

The acceleration ageing factor is derived from conductor failure history, cross referenced with the predicted failures. The acceleration curve should be applicable to each of the corrosion categories C1-C5 (ISO 9223 and ISO 9226). The material degeneration acceleration factor is different for each material, when considering composite materials such as ACSR conductor and galvanised steel shield wire. For the simplicity of calculation, the accelerating ageing factor will be calculated as a combined value for the zinc and carbon steel in 7/3.35 shield wire and a combination if the Aluminium, Zinc and Carbon Steel in Wolf ACSR conductor. Table 3-4 shows the ratio of aluminium degeneration for measured and predicted values for Wolf ACSR conductor measured between 18 and 38 years in a category C4 corrosion environment [106] while figure 3-8 shows the derived ageing logarithmic equation.

Table 3-4 Data for the conductor Ageing Acceleration calculation

| Line Name | Age of Line | Corrosion Category | Predicted Annual loss of Galvanised Steel ($\mu\text{m}/\text{year}$) | Total Predicted loss of Galvanised Steel ($\mu\text{m}/\text{year}$) | Total Measured Loss of Galvanised Steel ($\mu\text{m}/\text{year}$) | Difference between Measured and Predicted ($\mu\text{m}/\text{year}$) | m | Average | X |
|--------------------------|-------------|--------------------|---|--|---|---|-------------|-------------|-----------|
| Sub transmission Line 1 | 18 | C4 | 525 | 9450 | 11200 | -1750,00 | -0,15625000 | -0,15625000 | 0,8553453 |
| Sub transmission Line 2 | 22 | C4 | 525 | 11550 | 14200 | -2650,00 | -0,18661972 | -0,18661972 | 0,8297592 |
| Sub transmission Line 3 | 23 | C4 | 525 | 12075 | 15900 | -3825,00 | -0,24056604 | -0,24056604 | 0,7861827 |
| Sub transmission Line 4 | 29 | C4 | 525 | 15225 | 17800 | -2575,00 | -0,14466292 | -0,12715602 | 0,8805963 |
| Sub transmission Line 5 | 29 | C4 | 525 | 15225 | 17100 | -1875,00 | -0,10964912 | | |
| Sub transmission Line 6 | 32 | C4 | 525 | 16800 | 17600 | -800,00 | -0,04545455 | -0,04545455 | 0,955563 |
| Sub transmission Line 7 | 34 | C4 | 525 | 17850 | 19600 | -1750,00 | -0,08928571 | -0,12562877 | 0,8819422 |
| Sub transmission Line 8 | 34 | C4 | 525 | 17850 | 21300 | -3450,00 | -0,16197183 | | |
| Sub transmission Line 9 | 36 | C4 | 525 | 18900 | 24100 | -5200,00 | -0,21576763 | -0,21576763 | 0,8059225 |
| Sub transmission Line 10 | 37 | C4 | 525 | 19425 | 23600 | -4175,00 | -0,17690678 | -0,17690678 | 0,8378579 |
| Sub transmission Line 11 | 38 | C4 | 525 | 19950 | 24800 | -4850,00 | -0,19556452 | -0,20229419 | 0,8168546 |
| Sub transmission Line 12 | 38 | C4 | 525 | 19950 | 25222 | -5272,00 | -0,20902387 | | |

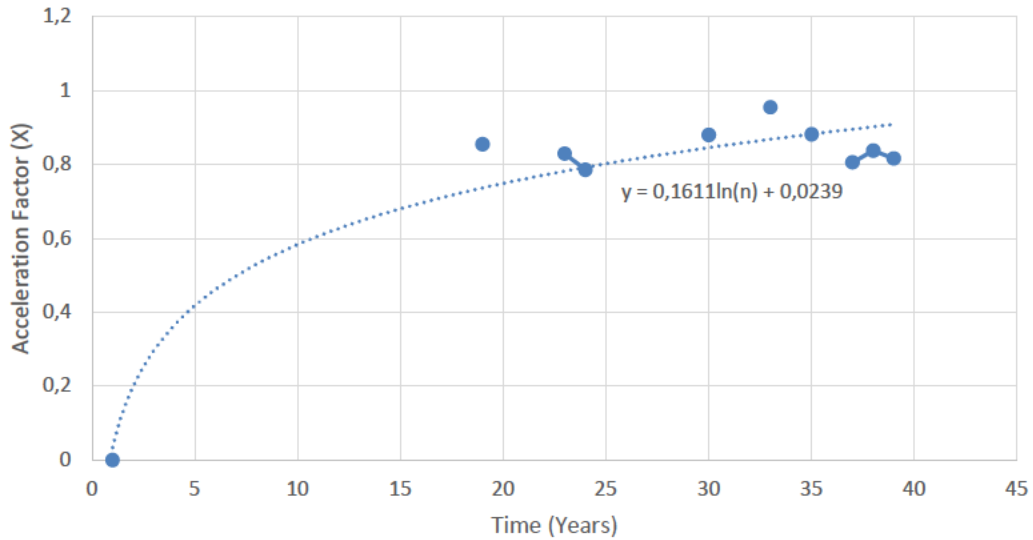


Figure 3-8 ACSR conductor Accelerated Ageing model (18 years)

Figure 3-9 shows the ageing acceleration curve for factor derived for a hundred-year period by utilizing the derived equation $y = 0.1611 \ln(n) + 0.0239$.

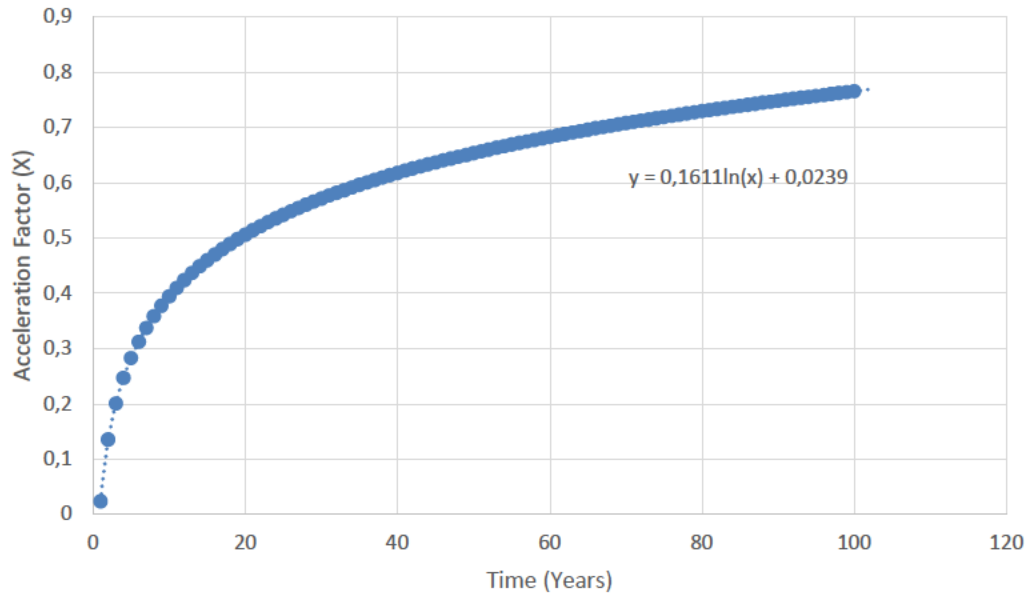


Figure 3-9 ACSR conductor Accelerated Ageing model (100 years)

Table 3-5 shows the ratio of galvanised steel shield wire degeneration for measured and predicted values measured between 17 and 47 years in a category C3 corrosion environment [106]. Figure 3-10 shows the graphical representation of the accelerated ageing for the 30-year period, while figure 3-11 shows the application of the derived ageing logarithmic equation over a hundred-year period.

Table 3-5 Data for the conductor Ageing Acceleration calculation

| Line Name | Age of Line | Corrosion Category | Predicted Annual loss of Aluminium (µm/year) | Total Predicted loss of Aluminium (µm/year) | Total Measured Loss of Aluminium (µm/year) | Difference between Measured and Predicted (µm/year) | n | Average | Y |
|--------------------------|-------------|--------------------|--|---|--|---|-------------|-------------|-----------|
| Sub transmission Line 1 | 17 | C3 | 1,5 | 25,5 | 50 | -24,50 | -0,96078431 | -0,96078431 | 0,3825927 |
| Sub transmission Line 2 | 18 | C3 | 1,5 | 27 | 40 | -13,00 | -0,48148148 | -0,15625000 | 0,8553453 |
| Sub transmission Line 3 | 22 | C3 | 1,5 | 33 | 50 | -17,00 | -0,51515152 | -0,22943723 | 0,7949809 |
| Sub transmission Line 4 | 29 | C3 | 1,5 | 43,5 | 70 | -26,50 | -0,60919540 | -0,49425287 | 0,6100265 |
| Sub transmission Line 5 | 29 | C3 | 1,5 | 43,5 | 60 | -16,50 | -0,37931034 | | |
| Sub transmission Line 6 | 37 | C3 | 1,5 | 55,5 | 90 | -34,50 | -0,62162162 | -0,62162162 | 0,5370728 |
| Sub transmission Line 7 | 41 | C3 | 1,5 | 61,5 | 80 | -18,50 | -0,30081301 | -0,30081301 | 0,7402162 |
| Sub transmission Line 8 | 44 | C3 | 1,5 | 66 | 90 | -24,00 | -0,36363636 | -0,36363636 | 0,6951439 |
| Sub transmission Line 9 | 44 | C3 | 1,5 | 66 | 80 | -14,00 | -0,21212121 | | |
| Sub transmission Line 10 | 44 | C3 | 1,5 | 66 | 100 | -34,00 | -0,51515152 | | |
| Sub transmission Line 11 | 47 | C3 | 1,5 | 70,5 | 100 | -29,50 | -0,41843972 | -0,41843972 | 0,6580728 |

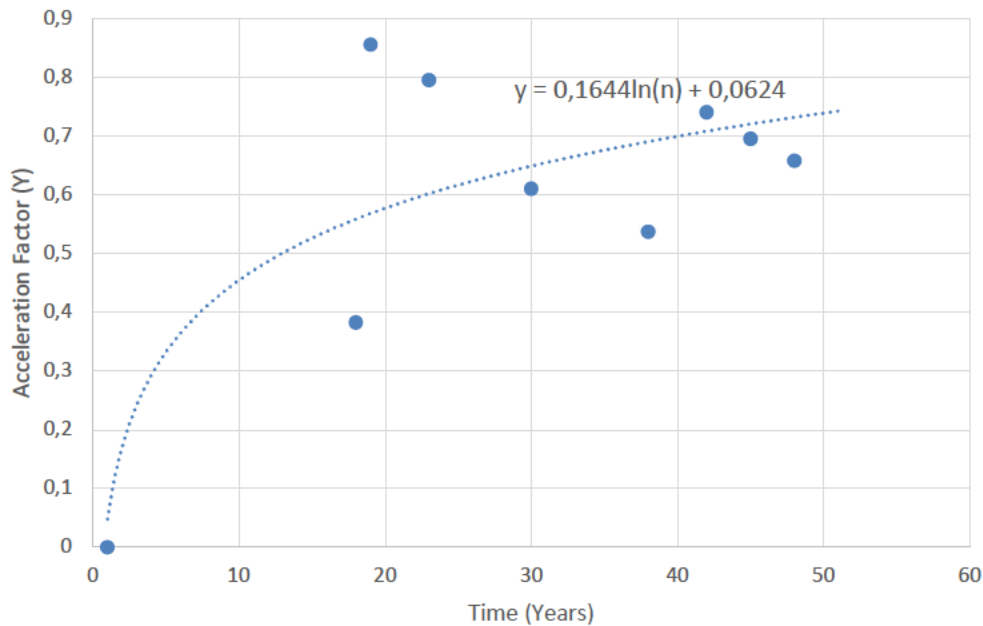


Figure 3-10 Shield wire Accelerated Ageing model (30 years)

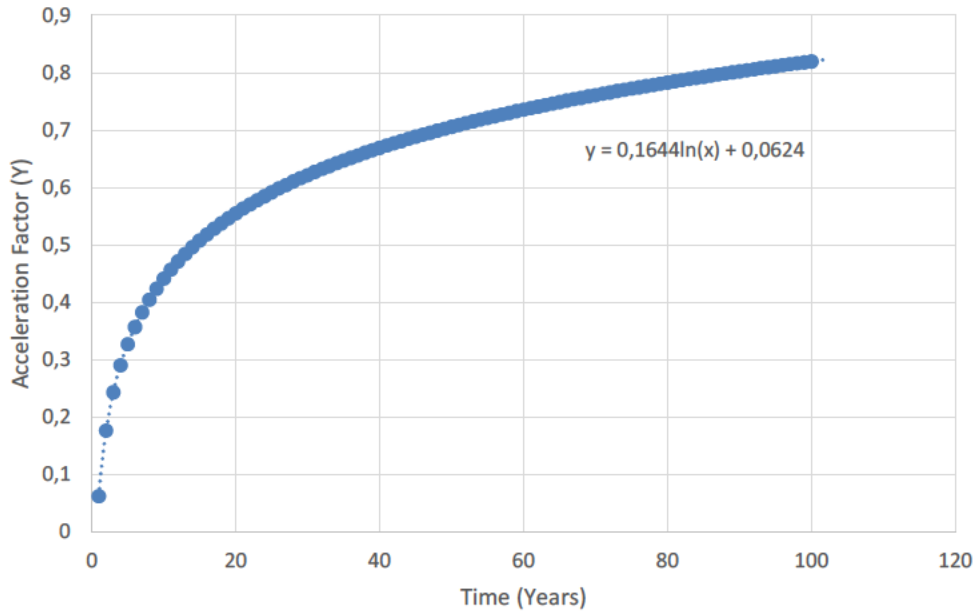


Figure 3-11 Shield wire Accelerated Ageing model (100 years)

3.3.2 Conductor Ageing Model Validation

Eight ACSR conductor samples were analysed from different corrosion categories, namely C2 to C5, specific to five Wolf conductor and two Bear conductor samples with an installation range of 26 to 47 years. The individual strand tensile strength was tested for steel tensile strength according to IEC 888 [107] and Aluminium tensile strength according to IEC 889 [108].

The seven samples were modelled using equation 3.5 to determine the material degeneration for the first year, the calculation limited to the outer layer of aluminium strands due to the presence of grease on the inner strands. The annual monthly temperatures and humidity values were secured from weather stations positioned near the line routes [109-115]. The galvanizing and steel core is taken at 100% UTS as the inner cores are not susceptible to the effects of corrosion due to the presence of conductor grease as verified by test results [116-123].

The two of the seven samples were compared to draw a conclusion. The Wolf samples were secured from different geographical areas, with varying offshore wind patterns, tower heights and sun shading. Figure 3-8 shows the resultant corrosion rates, which was at almost matched during the dry, low temperature winter period, however differed during the summer periods September to March. Considering that the contamination rates utilized are similar, both for chlorides and sulphur dioxide, the determine factors in the corrosion rates are mainly attributed to temperature and humidity. The rate of monthly corrosion is graphically represented in figure 3-12 and shown in table 3-6.

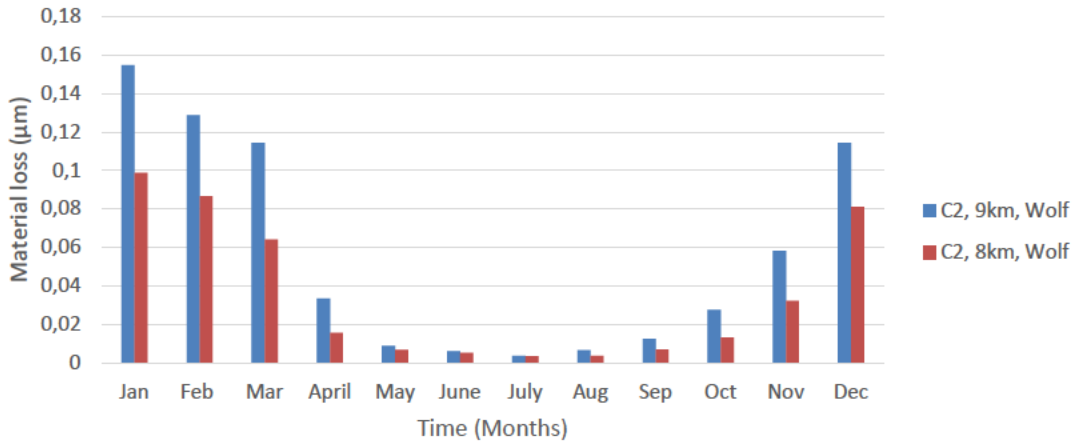


Figure 3-12 Graphical representation of first year Aluminium strand loss for Wolf ACSR conductor samples

Table 3-6 Data used for the first year Aluminium strand area loss calculation, for Wolf ACSR conductor samples

| C2, 9km, Wolf | Jan | Feb | Mar | April | May | June | July | Aug | Sep | Oct | Nov | Dec |
|-----------------------------|--------|-------|-------|-------|-------|-------|-------|-------|-------|-------|-------|--------|
| $T (^{\circ}C)$ | 25.28 | 25.28 | 24.17 | 21.94 | 19.72 | 17.78 | 17.78 | 18.89 | 20.56 | 21.67 | 22.50 | 24.44 |
| SO ₂ | 1.07 | 1.07 | 1.07 | 0.27 | 0.27 | 0.27 | 0.27 | 0.27 | 0.27 | 0.54 | 1.07 | 1.07 |
| RH (%) | 66.00 | 70.00 | 70.00 | 25.00 | 5.00 | 1.00 | 0.00 | 1.00 | 3.00 | 18.00 | 43.00 | 60.00 |
| $f_{AL} 0.043(T-10)$ | -0.66 | -0.66 | -0.61 | -0.51 | -0.42 | -0.33 | -0.33 | -0.38 | -0.45 | -0.50 | -0.54 | -0.62 |
| Cl (mg/(m ² .d)) | 103.52 | 72.46 | 51.76 | 31.06 | 20.70 | 20.70 | 10.35 | 10.35 | 20.70 | 31.06 | 51.76 | 103.52 |
| R _{corr} (µm) | 0.10 | 0.09 | 0.06 | 0.02 | 0.01 | 0.01 | 0.00 | 0.00 | 0.01 | 0.01 | 0.03 | 0.08 |

| C2, 8km, Wolf | Jan | Feb | Mar | April | May | June | July | Aug | Sep | Oct | Nov | Dec |
|-----------------------------|-------|-------|-------|-------|-------|-------|-------|-------|-------|-------|-------|-------|
| $T (^{\circ}C)$ | 26.11 | 26.11 | 25.56 | 23.33 | 21.11 | 19.44 | 19.17 | 20.28 | 21.39 | 22.22 | 23.89 | 25.00 |
| SO ₂ | 1.07 | 1.07 | 1.07 | 0.27 | 0.27 | 0.27 | 0.27 | 0.27 | 0.27 | 0.54 | 1.07 | 1.07 |
| RH (%) | 86.00 | 80.00 | 84.00 | 50.00 | 15.00 | 2.00 | 0.00 | 3.00 | 10.00 | 33.00 | 58.00 | 76.00 |
| $f_{AL} 0.043(T-10)$ | -0.69 | -0.69 | -0.67 | -0.57 | -0.48 | -0.41 | -0.39 | -0.44 | -0.49 | -0.53 | -0.60 | -0.65 |
| Cl (mg/(m ² .d)) | 98.85 | 88.96 | 69.19 | 39.54 | 19.77 | 19.77 | 9.88 | 19.77 | 39.54 | 59.31 | 69.19 | 98.85 |
| R _{corr} (µm) | 0.16 | 0.13 | 0.11 | 0.03 | 0.01 | 0.01 | 0.00 | 0.01 | 0.01 | 0.03 | 0.06 | 0.11 |

Figure 3-13 shows the cumulative first year corrosion rates for the Wolf and Bear samples. The results are consistent with distance from a contamination source and wetting from the coast or water body, i.e., category C2 with a higher rate of corrosion than C5 which is further away from the contaminant and wetting source.

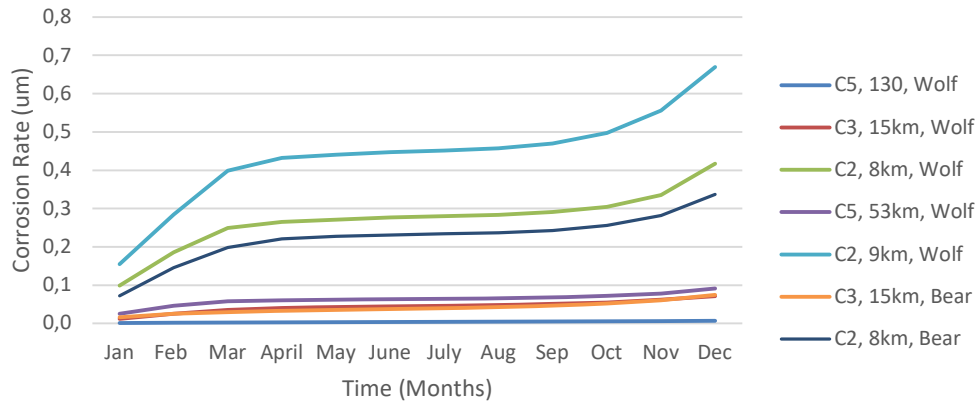


Figure 3-13 First year corrosion rate of Wolf and Bear samples

Based on the multi core configuration of the ACSR conductor samples, only outer strands were used in the calculation for corrosion material loss as, the conductor sample analysis showed that the contaminants and wetting had not impregnated the inner layers due to the presence of grease. The inner cores are assumed to possess a hundred percent of the installed tensile strength for the calculations. In certain instances, where the grease has leached out or, if three or fewer layered conductor is utilized, the second layer will be included in the corrosion equation after an estimated period.

Figure 3-14 shows the calculated tensile strength for the wolf and Bear conductor samples. The simulations start at $\pm 110\%$ as several conductor tests have shown that the tensile strength of the steel core at 15-20% higher than prescribed values. The class A galvanised steel wire was manufactured within recommended diameter, however the density of the steel proved to account for the higher manufacturing strength. The Wolf conductor samples within the C2 categories, suffered significant degeneration attributed mainly to one of four layers being subjected to the effects of corrosion. Bear conductor within the same C2 environment showed a lower degeneration rate due to the effects of corrosion on only one of the five layers. The projected 95% of UTS for Wolf conductor within in a C2 corrosion category, is reached within the 30–40-year period, based on the installation UTS, which is available from the manufacture as part of routine tests.

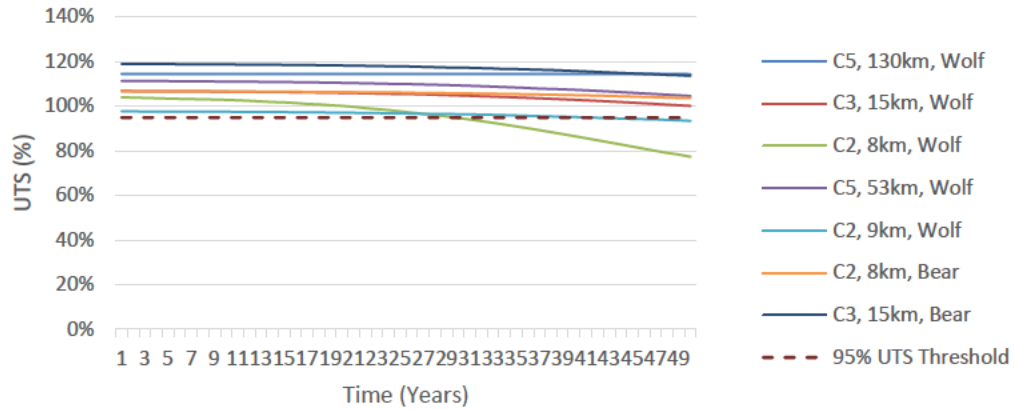


Figure 3-14 Calculated UTS loss for Wolf and BEAR samples

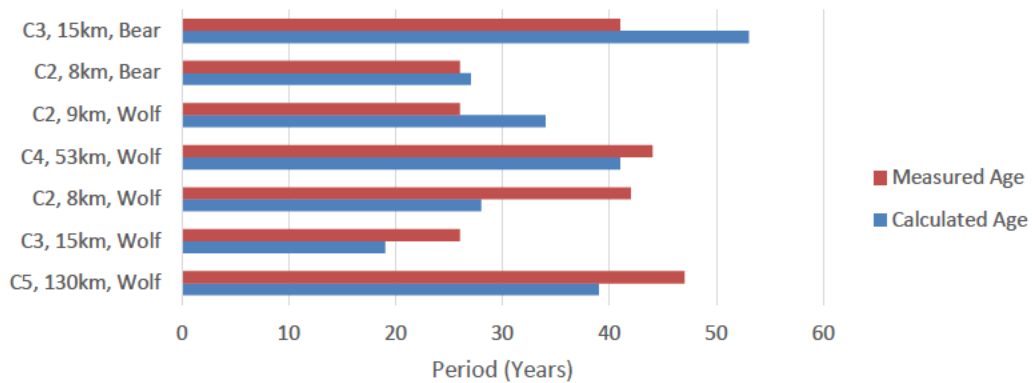


Figure 3-15 Measured and calculated age of Wolf and Bear samples

Figure 3-15 shows that the variance between the calculated values and the measured values, varied between 2 and 11 years. The variance is attributed to a higher contaminant and wetting rate due to specific wind conditions at certain sections of the line route. The standard deviation plot is shown in figure 3-16 where the average is 7.571 years and standard deviation is 4.577 years with an error of 1.868.

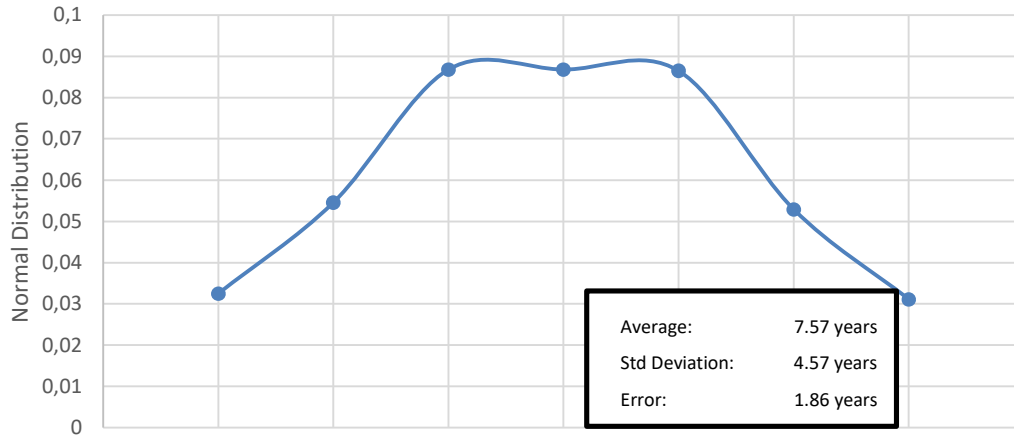


Figure 3-16 Standard deviation plot between measured and calculated life prediction

3.3.3 Shield Wire Ageing Model Validation

Six shield wire samples were selected from installed C2 and C3 corrosion categories, with a spread of the commonly installed double layered galvanised wire. The sample set was analysed at a mechanical strength testing facility to determine the ultimate strand strength, and metallogical properties of the zinc layer and steel.

The criteria utilized in the shield wire samples lifespan validation are as follows namely:

- Average Monthly Temperatures- The average temperatures take the ambient conditions into account mainly. The current carrying conductor temperature is not taken into account in the calculation and may contribute to additional corrosion loss.
- Average Monthly Chloride deposits- The chloride deposits are available as an average of deposits within the measuring station. The value of chloride deposition is based on wind direction, topography, seasonal and climatic conditions.
- Average Monthly Sulphur dioxide deposits- Sulphur dioxide rates may vary seasonally and annually based on the industrial activity within the area. These values can be increased to reflect the in-situ conditions that the line is experiencing if the information is available (figure 2-8).
- Average Monthly Humidity levels- Humidity level should not be confused with rainfall and humidity has a sufficient longer solution medium to that of rain. The rain dries after a short period or may wash the contaminants of the conductor surface [124-130].

The resulting loss of galvanising for the first year, utilizing equation 3.7 where $n=0.8$ [80], is shown in in table 3-7 [106] for two test cases, while the remaining test cases are shown graphically in figure 3-17.

Table 3-7 Data used for the first year Galvanised Steel strand material loss calculation

| C3, 40km, 19/2.65 Galvanised Steel | Jan | Feb | Mar | April | May | June | July | Aug | Sep | Oct | Nov | Dec |
|---|-------|-------|-------|-------|-------|-------|-------|-------|-------|-------|-------|-------|
| $T (^{\circ}C)$ | 21,39 | 21,67 | 20,56 | 17,50 | 14,72 | 12,22 | 11,39 | 12,50 | 13,61 | 16,39 | 18,33 | 20,56 |
| $SO_2 (mg/m^2d)$ | 1,07 | 1,07 | 1,07 | 1,07 | 1,07 | 1,07 | 1,07 | 1,07 | 1,07 | 1,07 | 1,07 | 1,07 |
| RH (%) | 63,00 | 65,00 | 56,00 | 35,00 | 16,00 | 1,00 | 0,00 | 0,00 | 2,00 | 14,00 | 30,00 | 51,00 |
| $f_{Zn} 0.071(T-10)$ | 0,81 | 0,83 | 0,75 | 0,53 | 0,34 | 0,16 | 0,10 | 0,18 | 0,26 | 0,45 | 0,59 | 0,75 |
| Cl- (mg/m ² d) | 82,63 | 82,63 | 44,07 | 33,05 | 11,02 | 11,02 | 11,02 | 16,53 | 22,03 | 33,05 | 66,10 | 82,63 |
| $R_{corr} (\mu m)$ | 0,73 | 0,80 | 0,48 | 0,18 | 0,06 | 0,03 | 0,03 | 0,04 | 0,05 | 0,09 | 0,19 | 0,45 |

| C2, 40km, 7/2.65 Galvanised Steel | Jan | Feb | Mar | April | May | June | July | Aug | Sep | Oct | Nov | Dec |
|--|--------|--------|--------|-------|--------|-------|-------|-------|--------|--------|--------|--------|
| $T (^{\circ}C)$ | 20,28 | 20,83 | 19,72 | 17,50 | 15,28 | 13,33 | 12,50 | 13,33 | 14,44 | 15,83 | 16,94 | 19,17 |
| $SO_2 (mg/m^2d)$ | 1,07 | 1,07 | 1,07 | 1,07 | 1,07 | 1,07 | 1,07 | 1,07 | 1,07 | 1,07 | 1,07 | 1,07 |
| RH (%) | 78,00 | 83,00 | 72,00 | 38,00 | 6,00 | 2,00 | 2,00 | 2,00 | 10,00 | 13,00 | 42,00 | 67,00 |
| $f_{Zn} 0.071(T-10)$ | 0,73 | 0,77 | 0,69 | 0,53 | 0,37 | 0,24 | 0,18 | 0,24 | 0,32 | 0,41 | 0,49 | 0,65 |
| Cl- (mg/m ² d) | 121,37 | 105,18 | 145,64 | 64,73 | 129,46 | 16,18 | 16,18 | 48,55 | 890,01 | 121,37 | 121,37 | 121,37 |
| $R_{corr} (\mu m)$ | 1,23 | 1,54 | 0,96 | 0,22 | 0,12 | 0,04 | 0,04 | 0,06 | 0,29 | 0,13 | 0,28 | 0,75 |

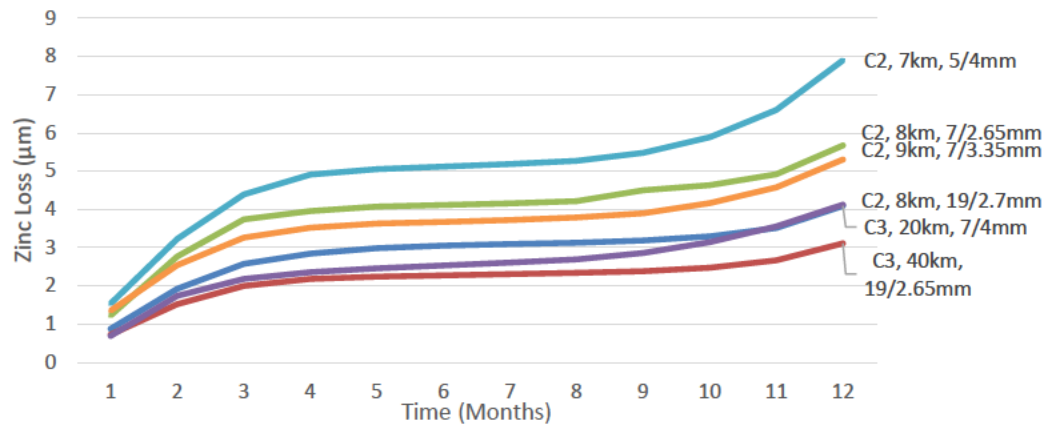


Figure 3-17 Loss of galvanizing on the outer cores of the various shield wires for the first year

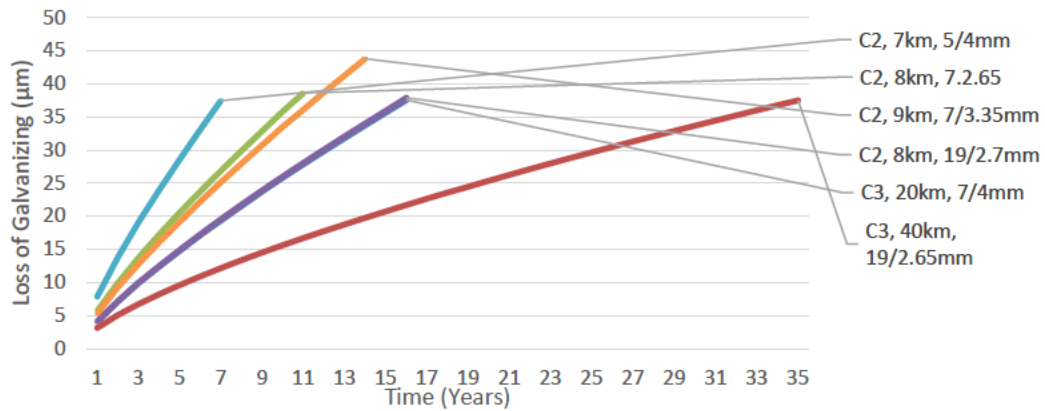


Figure 3-18 Loss of galvanizing on the outer cores of the various shield wires

The loss of the shield wire UTS is calculated by applying equation 3.7 to determine the first-year galvanizing corrosion loss. The galvanizing corrosion loss is linear, resulting in the exposure of the steel in the outer cores once the galvanizing layer has eroded [131-133], the inner strands of the shield wire are rated at one hundred percent for the calculations. Equation 3.6 is used to determine the first-year corrosion rate of the steel cores, and the acceleration factor is applied ($y = 0.218 \ln(n) - 0.2172$). The resulting loss of conductor strength of the six sampled are shown in figure 3-18.

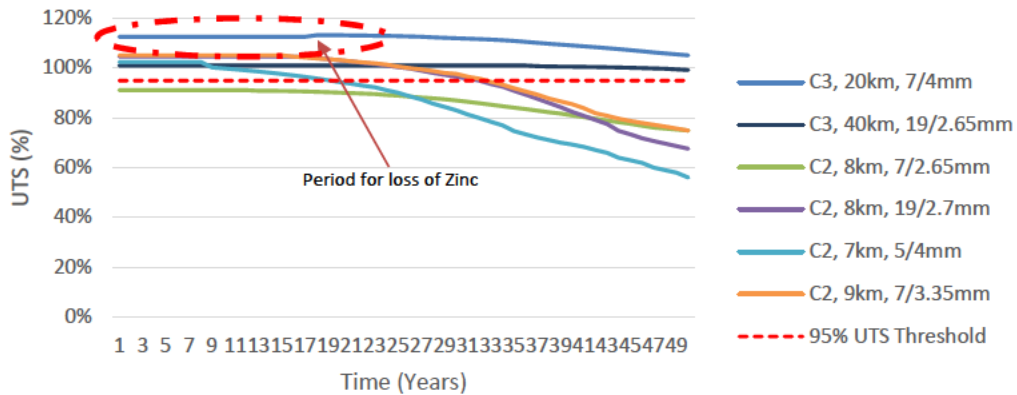


Figure 3-19 Calculated UTS loss for the various shield wire samples

The calculated UTS of the sample shield wires are shown in Figure 3-19. The initial degeneration of each shield wire type, is represented by a flat line on the graph, indicating the linear loss of galvanising. Once the galvanizing layer is lost, steel surface area is lost resulting in the loss of UTS of the composite shield wire. The time taken to reach 95% UTS in a C2 corrosion category is within 33 years while a C3 corrosion shield wire may be in operation beyond 50 years while maintaining its 95% UTS integrity.

In the case of C3, 20km, 7/4mm shield wire, the galvanizing layer is lost over a 17-year period, delaying material loss on the steel strands. In the case of C2, 7km, 5/4mm shield wire, the galvanizing layer is lost in 9 years and the strands deteriorate rapidly due to a larger exposed surface area i.e., single layered. One of the samples tested, namely, C2, 8km, 7/2.65mm showed that the conductor had defects when installed, not attaining the sub minimum rated tensile strength [134-139].

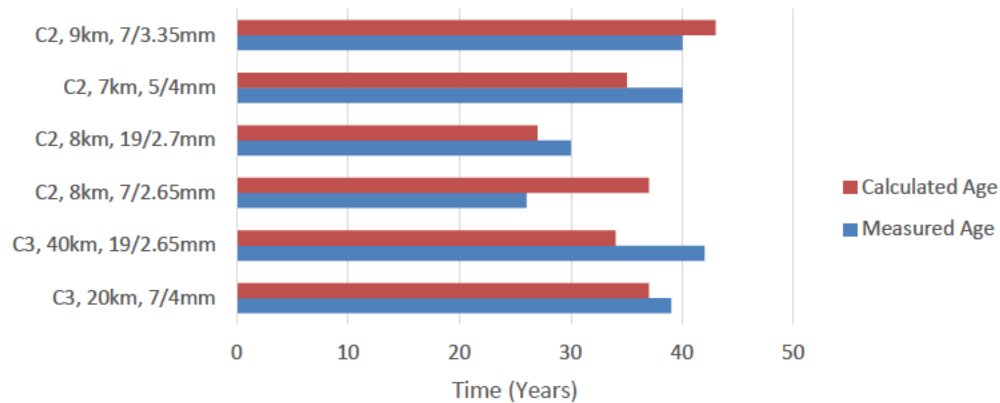


Figure 3-20 Variance between the calculated and measured age prediction of the various shield wires

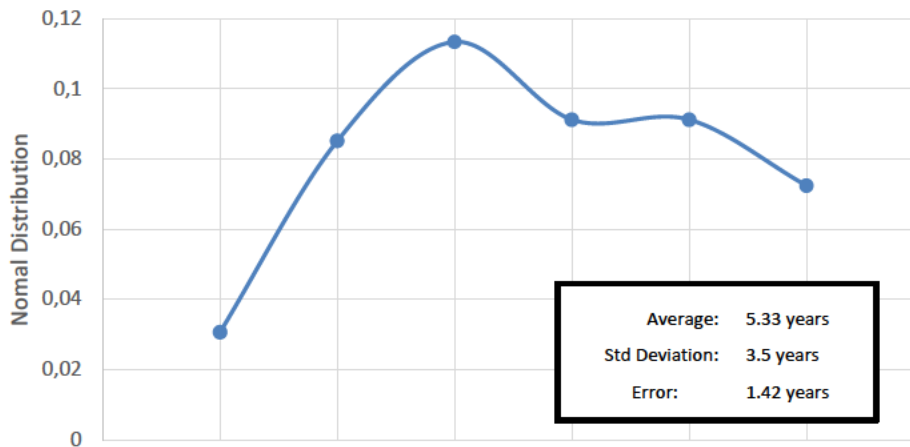


Figure 3-21 Standard deviation plot between the calculated and measured shield wire samples

Figure 3-21 shows a standard deviation of 3.5 years, an average of 5.33 years and an error of 1.4 years between the measured and calculated values for the six shield wire samples. The variance between the calculated and measured values (figure 3-20) may be attributed to the average values used for monthly for the temperature, sulphide deposits or humidity, which is acquired from area weather stations. Specific

measured values may yield more closely matched correlations between the measured and calculated values. It is also interesting to note that the six samples tested, showed a higher year one yield strength than the prescribed minimum as per ISO 9223, in some cases, the yield strength was 10% higher than the minimum prescription.

3.4 Summary

Assets management requires the ageing behaviour of components and systems to be effectively modelled in order for asset management principles to be applied. Ageing functions such as the Arrhenius Weibull and power law, may be utilized to predict the ageing effect by taking cognisance of material properties degeneration or external factors into account, such as environmental conditions.

In modelling of silicone composite insulation, the contamination flashover is mainly attributed to the loss of insulator surface resistance, influenced by the effects of environmental conditions. The effects of high contamination environments have a proportionally high flashover rate, wetting and contamination being the primary contributing factors to flashovers within coastal environments.

Atmospheric corrosion is the primary contributor to aluminium, and steel corrosion in coastal environments where, humidity and contaminants are available in abundance. Aluminium corrosion rate is lower than that of steel corrosion for ACSR conductor however, if conductor grease between successive strand layers were to be weathered, the resulting loss of tensile strength may be significantly speed up. Fortunately, the ACSR conductor mechanical strength lies with the steel core which is protected by several layers of aluminium as well as conductor grease which impairs contamination impregnation. The galvanised steel shield wire, however, is susceptible to the effects of atmospheric corrosion, which is retarded by the galvanizing layer. The power law provides the accelerating factor for material degeneration, in the various coastal environments.

CHAPTER 4 CONCLUSION

Sub transmission line systems are comprised of several electrical and mechanical components, the electrical components being the conductor, insulation, and grounding systems (shield wire). The mechanical components that support the conductor are the tower steelwork, the attachment hardware, and the foundations. The impact of electrical ageing failure is common, and the effects are short of catastrophic resulting in economic impacts as well as safety impacts. Tower steel, and foundations have a higher factor of redundancy incorporated into the initial designs to account for a multitude of conductor configurations and is excluded from the study area.

Insulator ageing is predominantly attributed to environmental influences which include ultraviolet radiation, temperature, precipitation, altitude, and atmospheric contaminants. Whilst lightning, altitude and UV radiation are of secondary concern in coastal environments, temperature, precipitation, and contaminants significantly influence the performance of silicone composite insulators. Ageing of insulators is attributed to the weakening of the resistive properties of the insulator surface which leads to a flashover and is represented by the loss of hydrophobicity. The fitting model that represents the loss of resistive properties of insulation is the Obenaus model, which represents an electrical circuit model of the arc propagation along the insulator surface. Rizk and Holtzhausen provides voltage flashover model that incorporates that conductance values of the solution on the insulator surface as well as creepage values. Unfortunately, the model is confined to predicting the voltage flashover for a specific creepage value and in the age process, however creepage values degenerate due to weathering of the insulator surface. The yearly degeneration of the insulator surface resistance is represented by the Arrhenius probability distribution plot, resulting in an acceleration factor that can be applied to the various contamination categories and specific to the material properties of silicone.

The proposed insulator ageing model was tested against in-situ failed insulator results specifically in a high contamination and high wetness environment. There was a correlation between the predicted and calculated results, the average is 2.125 years and standard deviation is 4.286 years. The variance in the measured and calculated values is due to higher ESDD rate on the insulator surface due to specific wind conditions at certain towers. Additionally, the loss of the ATH fillers over a period, has also contributed to the formation of pores, cracks, and crevices, which was incorporated into the loss of surface resistance model.

Atmospheric corrosion has contributed significantly to the ageing of aluminium and steel, especially in coastal environments where humidity and contaminants are available in large quantities. Corrosion of ACSR conductor acts on the outer layer initially and impregnates the inner layers as the conductor grease becomes non effective. Similarly, the galvanised steel shield corrosion process begins with loss of galvanizing on the outer surface of the outer of the steel wire, irrespective if the conductor grease is present. Once the galvanising layer is eroded, the strands erode in the chemical process resulting in loss of tensile

strength of the conductor. The second stage occurs directly after the galvanizing layer is lost, and the steel strands begin to corrode.

Modelling of the ageing behaviour of ACSR conductor and galvanised steel shield wire based on the degeneration of Aluminium, Zinc and Steel in five corrosive environments. ISO 9233 provides the empirical equation for the various material degeneration for the first year of degeneration, however, for an ageing behaviour to be simulated, an acceleration factor is required. The acceleration factor is calculated utilizing the power law while incorporating in-situ failure data. Corrosion categories C1-C5 can apply the acceleration factor to determine the material loss, both for steel and aluminium.

Several ACSR conductor samples from various C2 to C5 corrosion categories, were tested for mechanical tensile strength. The results revealed that there is a close correlation between the measured samples and the calculated values, varying between a minimum of 2 years and a maximum of 11 years. The variance in the measured and calculated values is attributed to higher contaminant and wetting rate on that conductor sample due to specific wind conditions at certain sections of the line route. Towers that are in the direct open-air path of the offshore winds are susceptible to a higher rate of corrosion, resulting in short lifespan. Wind patterns and moisture levels contribute to the corrosion rate however, as seen with multilayer conductor such as Bear conductor, corrosion of the outer cores minimally affects the structural integrity of the composite conductor, provided that the conductor grease remains intact. The standard deviation of 4.577 years, an average of 7.571 years and an error of 1.868 was calculated.

The shield wire material degeneration as modelled on a linear degeneration of the zinc on the galvanizing layer based on the first-year degeneration rate, for the six samples. A standard deviation of 0.5 years, an average of 5.33 years and an error of 1.4 years between the measured and calculated values for the six shield wire samples was concluded, thereby proving validity of the model. The variance between the calculated and measured values may be attributed to the average values used for monthly for the temperature, sulphide deposits or humidity, which is acquired from area weather stations. Specific measured values may yield more closely matched correlations between the measured and calculated values. It is also interesting to note that the six samples tested, showed a higher year one yield strength than the prescribed minimum as per ISO 9223, in some cases, the yield strength was 10% higher than the minimum prescription.

The prediction models for silicone composite insulators, steel shield wire and ACSR conductor show a close correlation between measured and calculated values, governed by the accuracy of the environmental conditions at the specific point of the sub transmission lines being measured. Additionally, conductor and shield wire, samples have shown to provide a higher than recommended minimum tensile rating when new, distorting the calculated end of life. Therefore, new samples require testing when installed to effectively predict the useful life without prematurely disposing of the conductor as it ages. The prediction model has

also shown that in some cases, the lifespan recommended in NRS-093-1, is not achievable, especially in harsh coastal conditions, warranting further material research for those specific applications.

Finally, from an asset management perspective, once the component lifespan is determined, the system lifespan can be determined. It is evident from the research that ACSR conductor and galvanised steel wire should not be installed in a C1-C2 corrosion category and similarly composite insulators should not be installed in a E5-E7 contamination category due to premature failure. Historically recurring conductor and insulator failures within these environments were recorded as maintenance, installation or manufacturing related failures, however the asset manager can now, conclusively deduce that the component has achieved the intended design lifespan and should be replaced. Additionally, the asset manager is able to adequately plan in terms of the amount of maintenance related failures to anticipate as the conductor failures increase or for the planning of spare insulator as they fail. Financially, funding models may be submitted with confidence substantiating the replacement, refurbishment, or differing investment in the asset.

In both cases of insulator and conductor ageing, the static parameters are the material ageing defined by predictable degeneration of the silicon layer and the that of aluminium or steel. The dynamic parameter is the ageing acceleration factor which is dependant on several asset management risk indices that determine the acceptable failure rates. Additionally, the failure history of the sub transmission lines in a contamination environment, drastically influence the acceleration ageing factor. Ultimately, component sampling and testing aides in the refinement the ageing model. The acceleration factor is dependant on the number of lines being analysed, the greater the number of line data available, the smother the exponential function and smaller the margin of error. Also, the predicted failure values compiled in the asset management strategy for the useful life of lines within certain corrosion categories, are far too conservative than actual measurements, resulting in unanticipated system failures.

BIBLIOGRAPHY

- [1] D. Asija, and R. Viral, “*Chapter 13 - Renewable energy integration in modern deregulated power system: challenges, driving forces, and lessons for future road map*”, Advances in Smart Grid Power System, Academic Press, 2021, Pages 365-384. ISBN 9780128243374, <https://doi.org/10.1016/B978-0-12-824337-4.00013-8>.
- [2] ISO 55000:2014, “*Asset management - Overview, principles and terminology*”.
- [3] ISO 9223:2012, “*Corrosion of metals and alloys - Corrosivity of atmospheres, Classification, determination and estimation*”.
- [4] T. Salunkhe, N. Jamadar and S. Kivade, “*Prediction of Remaining Useful Life of Mechanical Components-A Review*”, International Journal of Engineering Science and Innovative Technology (IJESIT), 2014, vol. 3, no. 6, pp. 125-130. ISSN: 2319-5967.
- [5] U. Minnaar, W. Visser and J. Crafford, “*An economic model for the cost of electricity service interruption in South Africa*”, Utilities Policy, vol. 48, 2017, pp. 41-50, Available: 10.1016/j.jup.2017.08.010.
- [6] W. Vasquez, and D. Jayaweera, “*Methodology for Overhead Conductor Replacement Considering Operational Stress and Aging Characteristics*”, 2018, pp. 1-5. Available: 10.1109/PESGM.2018.8586012.
- [7] PAS 55-1:2008, “*Asset management, Part 1: Specification for the optimized management of physical assets*”.
- [8] D. Maletic, M. Maletic, B. Al-Najjar and B. Gomiscek, “*An Analysis of Physical Asset Management Core Practices and Their Influence on Operational Performance*”, Sustainability, 2020, vol. 12, no. 21, pp. 90-97. Available: 10.3390/su12219097.
- [9] W. Li, “*Evaluating mean life of power system equipment with limited end-of-life failure data*”, IEEE Trans. Power Syst., 2004, vol. 19, no. 1, pp. 236–242.
- [10] J. Endrenyi, “*Reliability and maintenance*”, in IEEE Tutorial Text on Electric Delivery Systems Reliability Evaluation, Ch. 5., 2005 IEEE PES General Meeting, San Francisco, CA, June 2005, Ch. 5, Tutorial 05TP175.

- [11] L. Wenyuan, E. Vaahedi, E. and P. Choudhury, "Power system equipment ageing", Power and Energy Magazine, IEEE. 4. 52 - 58. 10.1109/MPAE.2006.1632454.
- [12] W. Li, "Incorporating aging failures in power system reliability evaluation", IEEE Trans. Power Syst., vol. 17, no. 3, pp. 918–923, Aug. 2002.
- [13] J. Oakland, "Total Quality Management", 2nd ed. Oxford: Butterworth-Heinemann, 2014, pp. 113-116.
- [14] M. Buhari and S. Awadallah, "Modelling of Ageing Distribution Cable for Replacement Planning", Power Systems, 2015, IEEE. 1. 10.1109/TPWRS.2015.2499269.
- [15] O. Caxton et al., "Overview of remaining useful life prediction techniques in Through-life Engineering Services", 2014, Procedia CIRP. 16. 158–163. 10.1016/j.procir.2014.02.006.
- [16] NRS 093-1, "Asset Management of Electricity Infrastructure: Asset Management of Electricity Infrastructure Part 1: Minimum requirements for asset management in the South Africa Electricity Distribution Industry ", Edition 1, 2009.
- [17] J. Butler, "The Evolution of Transmission and Distribution Insulators", Utilityproducts.com, 2021. [Online]. Available: <https://www.utilityproducts.com/magazine/61611>. [Accessed: 18- Dec- 2021].
- [18] EPRI, "Overhead Transmission Inspection, Assessment, and Asset Management Reference Guide", EPRI- Palo Alto, CA, Tech., Report No. 3002003603, 2014, pp. 65-78.
- [19] H. Hillborg, "Loss and Recovery of Hydrophobicity of polydimethylsiloxane after exposure to electrical discharges", Diva-portal.org, 2001. [Online]. Available: <http://www.diva-portal.org/smash/get/diva2:8835/FULLTEXT01.pdf>. [Accessed: 13- Jan- 2021].
- [20] R. E. Macey, W. Vosloo and C. Turreil, "The practical guide to outdoor high voltage insulators" Johannesburg SA, Crown Publications, 2004, pp. 34-80.
- [21] EPRI, "Insulator Reference Book", Palo Alto, CA, Tech. Report No. 3002010140, 2017, pp. 23-43.
- [22] L. Cheng, L. Wang, Z. Guan and F. Zhang, "Aging characterization and lifespan prediction of silicone rubber material utilized for composite insulators in areas of atypical warmth and humidity", IEEE Transactions on Dielectrics and Electrical Insulation, 2016, vol. 23, no. 6, pp. 3547-3555. Available: 10.1109/tdei.2016.005784.

- [23] IEC 62217, "Polymeric insulators for indoor and outdoor use with a nominal voltage >1 000 V – General definitions, test methods", standard edition 1.0, 2.0., 2005.
- [24] M. Daud, P. Ciufu and S. Perera, "A study on the suitability of cable models to simulate switching transients in a 132 kV underground cable", Australian Journal of Electrical & Electronics Engineering, vol. 10, no. 1, 2013 pp. 221-224. Available: 10.7158/e11-037.2013.10.1.
- [25] W. Diesendorf, "Insulation Co-ordination in High Voltage Electric Power Systems", Butterworth and Co Ltd., 1974, pp. 141-173.
- [26] J. Das, "Transients in electrical systems", 1st ed. New York: McGraw-Hill, 2010, pp. 312-367.
- [27] R. Degeneff, W. McNutt, W. Neugebauer, J. Panek, M. McCallum and C. Honey, "Transformer Response to System Switching Voltages", IEEE Power Engineering Review, 1982, vol. -2, no. 6, pp. 34-35. Available: 10.1109/mper.1982.5520987.
- [28] IEC 60071-2:1996, "Insulation co-ordination, Part 2: Application guide".
- [29] M. Gijben, "The lightning climatology of South Africa", South African Journal of Science, 2012, vol. 108, no. 34. Available: 10.4102/sajs.v108i3/4.740.
- [30] IEC 60507:1991, "Artificial Contamination Tests on High Voltage Insulators to Be Used on AC Systems".
- [31] J. Xingliang, W. Shaohua, Z. Zhijin, H. Jianlin and H. Qin, "Investigation of flashover voltage and non-uniform contamination correction coefficient of short samples of composite insulator intended for ± 800 kV UHVDC", IEEE Trans. Dielectric. Electr. Insul., 2010, vol. 17, pp. 71-80.
- [32] J. Xingliang, S. Lichun, Z. Yongji, Z. Zhijin and H. Jianlin, "Influence of ESDD and NSDD on AC flashover characteristic of artificially contaminated XP-160 insulators", Proceedings of the CSEE, 2006, vol. 26, pp. 24-28.
- [33] A. Vlastos and T. Orbeck, "Outdoor leakage current monitoring of silicone composite insulators in coastal service conditions", IEEE Transactions on Power Delivery, 1996, vol. 11, no. 2, pp. 1066-1070. Available: 10.1109/61.489369.
- [34] J. George and S. Prat, "Insulators under Fire", International conference on overhead lines, Design, Construction, Inspection & Maintenance, Fort Collins, Colorado, USA, 2019.

- [35] B. Chudnovsky, *“Electrical power transmission and distribution- Ageing and Life Extension Techniques”*, 1st ed. Boca Raton, FL: Taylor & Francis, 2013, pp. 215-234.
- [36] IEC 60815-1, *“Selection and Dimensioning of High-Voltage insulators intended for use in Contaminated Conditions- part 1: definitions, Information and General Principles”*, Version 1.0, 2009.
- [37] A. Nekahi, S. McMeekin and M. Farzaneh, *“Flashover Characteristics of Silicone Rubber Sheets under Various Environmental Conditions”*, *Energies*, 2016, vol. 9, no. 9, p. 683. Available: 10.3390/en9090683.
- [38] R. Gorur and R. Olsen, *“Prediction of Flashover Voltage of Insulators Using Low Voltage Surface Resistance Measurement”*, Pserc.wisc.edu, 2006. [Online]. Available: https://pserc.wisc.edu/documents/publications/reports/2006_reports/T-26G_Final-Report_Nov-2006.pdf. [Accessed: 22- Dec- 2020].
- [39] Arshad, A. Nekahi, S. McMeekin and M. Farzaneh, *“Flashover Characteristics of Silicone Rubber Sheets under Various Environmental Conditions”*, *Energies*, 2016, vol. 9, no. 9, p. 683. Available: 10.3390/en9090683.
- [40] W. Nel and P. D. Sumner, *“Intensity, energy and erosivity attributes of rainstorms in the KwaZulu-Natal Drakensberg, South Africa”*, *South African Journal of Science*, 2007, Vol. 103(9-10), pp. 398-402.
- [41] R. Taherian and A. Kausar, *“Electrical conductivity in polymer-based composites”*, 1st ed. E-book: William Andrew, 2018, pp. 135-175.
- [42] Z. Jiang et al., *“Investigating the Effect of Rainfall Parameters on the Self-Cleaning of Contaminated Suspension Insulators: Insight from Southern China”*, *Energies* 2017-10, 2017, pp. 601. <https://doi.org/10.3390/en10050601>
- [43] Cigre, *“The impact of rain on insulator performance”*, 2016. [Online]. Available: <https://e-cigre.org/publication/634-impact-of-rain-on-insulator-performance> [Accessed 04 March 2021].
- [44] IEC 60664-1, *“Insulation coordination for equipment within low-voltage systems - Part 1: Principles, requirements and tests”*, Ed. 2.0b, 2007.
- [45] INMR, *“Modern Contamination Monitoring Principles Allow Better Selection of Insulators for Contaminated Service Conditions (Part 1 of 2)”*, 2019, [online] Available at: <https://www.inmr.com/modern-contamination-monitoring-principles-allow-better-selection-insulators-contaminated-service-conditions-part-1-2/> [Accessed 28 April 2020]

- [46] W. Volsoo, and R. Swinny, "KIPTS Research Report 2006", Eskom resource and Strategy- Research Division, 2006, Report No. Res/RR/06/27792. [Online]. Available: <https://hyperwave.eskom.co.za> [Accessed: 06- Jan- 2020].
- [47] L. P. Grijalva and L. R. Talamas, "The Problem of Contamination on Insulators, *Journal of the Air Contamination Control Association*", 1979, vol. 29:12, pp. 1246-1247. DOI: 10.1080/00022470.1979.10470923
- [48] M. Hussain, M. Chaudhary and A. Razaq, "Mechanism of Saline Deposition and Surface Flashover on High-Voltage Insulators near Shoreline: Mathematical Models and Experimental Validations", *Energies*, 2019, vol. 12, no. 19, pp. 36-85. Available: 10.3390/en12193685.
- [49] L. Raffaele and L. Bruno, "Windblown sand action on civil structures: Definition and probabilistic modelling", *Engineering Structures*, 2019, vol. 178, pp. 88-101. Available: 10.1016/j.engstruct.2018.10.017.
- [50] Y. Hao, Y. Feng and J. Fan, "Experimental study into erosion damage mechanism of concrete materials in a wind-blown sand environment", *Construction and Building Materials*, 2016, vol. 111, pp. 662-670. Available: 10.1016/j.conbuildmat.2016.02.137
- [51] N. Mavrikakis, P. Mikropoulos and K. Siderakis, "Evaluation of field-ageing effects on insulating materials of composite suspension insulators", *IEEE Transactions on Dielectrics and Electrical Insulation*, 2017, vol. 24, no. 1, pp. 490-498. Available: 10.1109/tdei.2016.006077.
- [52] M. Mae et al., "Study of Tower Grounding Resistance Effected Back Flashover to 500 kV Transmission Line in Thailand by using ATP/EMTP", *International Journal of Electrical, Electronic and Communication Sciences*, 2008, vol2, issue 6, pp. 1112 – 1119. ISSN: 2517-9438
- [53] C. C. Brown, "Network planning guidelines for lines and cables: DST 34-619", *Eskom Intranet Eskom Distribution Technology*, Eskom Intranet, 2010. [Online]. Available: http://bits.eskom.co.za/bits/dtechsec/distribu/tech/GUIDE/DGL_34-619.pdf. [Accessed: 30- Dec- 2019].
- [54] Z. Zhang, X. Jiang, Y. Chao, L. Chen, C. Sun and J. Hu, "Influence of Low Atmospheric Pressure on AC Contamination Flashover Performance of Various Types of Insulators", *IEEE Transactions on Dielectrics and Electrical Insulation*, 2010, vol. 17, no. 2, pp. 171-178.

- [55] M. Abdelhalim, Z. Boubakeur and M. Belkheiri, "*Prediction of critical flashover voltage of contaminated insulators under sec and rain conditions using least squares support vector machines (LS-SVM)*", Diagnostyka, 2018, vol. 20, no. 1, pp. 49-54. Available: 10.29354/diag/99854
- [56] R. Sundararajan and R. W. Nowlin, "*Effect of altitude on the flashover voltage of contaminated insulators*", Proceedings of Conference on Electrical Insulation and Dielectric Phenomena - CEIDP '96, 1996, vol.2, pp. 433-436. doi: 10.1109/CEIDP.1996.564502.
- [57] B. Branfield, "*Determination of Conductor Ratings in Eskom- DST 32-319*", Eskom Intranet, 2010, [Online] Available: <https://hyperwave.eskom.co.za> [Accessed: 14- Jan- 2020].
- [58] B. Remy et al., "*Comparative Fatigue Resistance of Overhead Conductors Made of Aluminium and Aluminium Alloy: Tests and Analysis*", Procedia Engineering, 2015, Available: 133. 223-232. 10.1016/j.proeng.2015.12. 662.
- [59] ASTM, "*Annual book of ASTM standards- Copper and Copper Alloys*", 1st ed. West Conshohocken: ASTM International, 2009, pp. 327-414.
- [60] ASTM A475, "*Standard Specification for Zinc-Coated Steel Wire Strand*", 2003.
- [61] ASTM B230, "*Standard Specification for Aluminium 1350–H19 Wire for Electrical Purposes*", 2007.
- [62] R. Landolfo, L. Cascini and F. Portioli, "*Modelling of Metal Structure Corrosion Damage: A State-of-the-Art Report*", Sustainability, 2010, vol. 2, no. 7, pp. 2163-2175. Available: 10.3390/su2072163
- [63] C. Vargel, "*Corrosion of Aluminium*", 1st ed., Elsevier.com, 2004. [Online]. Available: <https://www.elsevier.com/books/corrosion-of-aluminium/vargel/978-0-08-044495-6> . [Accessed: 25- Nov- 2019]
- [64] S. Feliu and M. Morcillo, "*Corrosion in rural atmospheres in Spain*", British Corrosion Journal, 1987, vol 22:2, pp. 99-102. doi: 10.1179/000705987798271640
- [65] BS EN 50326:2002, "*Conductors for overhead lines. Characteristics of greases*", 2002.
- [66] G. de Leeuw et al., "*Production flux of sea spray aerosol*", Reviews of Geophysics, 2011, vol. 49, no. 2 pp. 12-18. Available: 10.1029/2010rg000349.
- [67] C. Borgmann, "*Initial Corrosion Rate of Mild Steel Influence of the cation*", Industrial & Engineering Chemistry, 1937, vol. 29, no. 7, pp. 814-821. Available: 10.1021/ie50331a018.

- [68] K. Hossain, and S. Easa, “*Spatial distribution of marine salts in coastal region using wet candle sensors*”, International Journal of Reviews and Applied Science, 2011, vol 7, pp. 228–235.
- [69] F. Corvo, N. Betancourt and A. Mendoza, “*The influence of airborne salinity on the atmospheric corrosion of steel*”, Corros. Sci., 1995, vol. 37, pp. 1889–1901, [https://doi.org/10.1016/0010-938X\(95\)00058-R](https://doi.org/10.1016/0010-938X(95)00058-R)
- [70] G. R. Meira, I. J. Padaratz, C. Alonso, and C. Andrade, “*Effect of distance from sea on chloride aggressiveness in concrete structures in Brazilian coastal site*”, 2003, Mater. Constr., vol 53, pp. 179–188.
- [71] S. Feliu, M. Morcillo and B. Chico, “*Effect of distance from sea on atmospheric corrosion rate*” Corrosion, 1999, vol. 55, pp. 883–891, <https://doi.org/10.5006/1.3284045>.
- [72] J. Alcantara, B. Chico, I. Diaz, D. de la Fuente and M. Morcillo, “*Airborne chloride deposit and its effect on marine atmospheric corrosion of mild steel*”, Corros. Sci., 2015, vol. 97, pp. 74–88, <https://doi.org/10.1016/j.corsci.2015.04.015>
- [73] M. Gobinddass, J. Molinie, S. Richard, K. Panechou, A. Jeannot and S. Jean-Louis, “*Coastal Sea Salt Chlorine Deposition Linked to Intertropical Convergence Zone (ITCZ) Oscillation in French Guiana*”, Journal of the Atmospheric Sciences, 2020, vol. 77, no. 5, pp. 1723-1731. Available: 10.1175/jas-d-19-0032.1.
- [74] O. Alao, “*Refinement of air-borne chloride exposure classes for RC structures in the Cape Peninsula*”, M.S. thesis, Dept. of Civil Engineering, University of Cape Town, 2015, pp. 145. [http://hdl handle net/11427/13644](http://hdl.handle.net/11427/13644).
- [75] A. Lourens et al., “*Spatial and temporal assessment of gaseous pollutants in the Highveld of South Africa*”, South African Journal of Science, 2011, vol. 107, no. 12. Available: 10.4102/sajs.v107i12.269
- [76] J. Martins, R. Dhammapala, G. Lachmann, C. Galy-LacauxI and J. Pienaar, “*Long term measurements of sulphur dioxide, nitrogen dioxide, ammonia, nitric acid and ozone in southern Africa using passive samplers*”, South African Journal of Science. sci., 2007, vol. 103, no. 7-8, pp. 336-342. Available: ISSN 1996-7489.
- [77] Energy and Clean Air, “*SO₂ Hotspots 2019*”, Energyandcleanair.github.io, 2021. [Online]. Available: https://energyandcleanair.github.io/202008_hotspots/. [Accessed: 30- Dec- 2021].
- [78] S. W. Dean, “*Natural Atmospheres: Corrosion*”, Encyclopaedia of Materials: Science and Technology, 2011, pp. 5930–5938. doi:10.1016/B0-08-043152-6/01033-0.

- [79] P.R. Roberge, "*Corrosion engineering: principles and practice*", McGraw-Hill New York, 2008, pp. 273-317.
- [80] R. Melchers, "*Predicting long-term corrosion of metal alloys in physical infrastructure*", npj Materials Degradation, 2019, vol. 3, no. 1, pp 73-81. Available: 10.1038/s41529-018-0066-x.
- [81] R. Melchers, "*Modelling of Marine Immersion Corrosion for Mild and Low-Alloy Steels—Part 2: Uncertainty Estimation*", Corrosion, 2003, vol. 59, no. 4, pp. 335-344. Available: 10.5006/1.3277565.
- [82] M. Schumacher, "*Seawater Corrosion Handbook*", 1st ed., Park Ridge New Jersey, William Andrews Publishing, 1979, pp. 374-387.
- [83] G. Tammann, "*Lehrbuch der metallographie: chemie und physik der metalle und ihrer legierungen*", Voss, 1923.
- [84] R. Melchers, "*Effect of temperature on the marine immersion corrosion of carbon steels*", Corrosion, 2002, vol 58, pp. 768-782.
- [85] A. Malik, P. M. Kutty, N. A. Siddiqi, I. N. Andijani, S. Ahmed, "*The influence of pH and chloride concentration on the corrosion behaviour of AISI 316L steel in aqueous solutions*", Corrosion science, 1992, vol. 33, pp. 1809-1827.
- [86] R. Melchers, "*Effect of immersion depth on marine corrosion of mild steel*", Corrosion, 5005, vol. 61, pp. 895-906.
- [87] H. Pham, "*Springer Handbook of Engineering Statistics*", 1st ed., New York: Springer, 2007, pp. 64-76.
- [88] F. Obenaus, "*Contamination flashover and creepage path length*", Dtsch. Elektrotechnik 1958, vol. 12, 135–136.
- [89] Q. Yang, R. Wang, W. Sima, C. Jiang, X. Lan and M. Zahn, "*Electrical Circuit Flashover Model of Contaminated Insulators under AC Voltage Based on the Arc Root Voltage Gradient Criterion*", Energies, 2012, vol. 5, no. 3, pp. 752-769. Available: 10.3390/en5030752.
- [90] C. Badachi and P. Dixit, "*Prediction of contamination flashover voltages of ceramic string insulators under uniform and non-uniform contamination conditions*", Journal of Electrical Systems and Information Technology, 2016, vol. 3, no. 2, pp. 270-281. Available: 10.1016/j.jesit.2016.01.003.

- [91] IMNR, "*Selecting Insulation for Overhead Lines & Substations in Russia*", 2018. [Online]. Available: <https://www.inmr.com/selecting-insulation-overhead-lines-substations-russia-2/>. [Accessed: 27- Jan-2022].
- [92] N. Vasudev, P. V. V. Nambudri, M. N. Dinesh, K. N. Ravi and V. Krishnan, "*Long term ageing performance of Silicone rubber insulators under different conditions*," 2009 IEEE 9th International Conference on the Properties and Applications of Dielectric Materials, 2009, pp. 276-280, doi: 10.1109/ICPADM.2009.5252431.
- [93] M. Gencoglu and M. Cebeci, "*The contamination flashover on high voltage insulators*", Electric Power Systems Research, 2008, vol. 78, no. 11, pp. 1914-1921. Available: 10.1016/j.epsr.2008.03.019.
- [94] F. A. M. Rizk, "*Mathematical Models for Contamination Flashover*", Electra, 1978, vol. 78, pp. 71-103.
- [95] J. P. Holtzhausen, "*Critical Evaluation of AC Contamination Flashover Models for HV Insulators having Hydrophilic surfaces*", PhD Thesis, University of Stellenbosch, South Africa, 1997, pp 63-76.
- [96] P. Claverie, "*Predetermination of behaviour of contaminated insulators*", IEEE Trans. Power App. Syst., 1971, vol. 90-4, pp. 1902-1908.
- [97] H. H. Woodson, A. J. Mcelroy, "Insulators with contaminated surfaces part II: modelling of discharge mechanisms", IEEE Trans. Power App. Syst., 1970, vol. 89-8, pp. 1858-1867.
- [98] Reliasoft Corporation, "*Accelerated life testing reference*", 6th ed. Tucson, Ariz.: ReliaSoft Publishing, 2001, pp. 30-56.
- [99] M Rashid, "*KZN Performance Data- 2008-2016*", Eskom KZN Plant Department Performance Data 2006-2016, Nov 2017. [Online]. <https://hyperwave.eskom.co.za> [Accessed: 17 May 2020].
- [100] M. Dong and A. Nassif, "*Combining Modified Weibull Distribution Models for Power System Reliability Forecast*", IEEE Transactions on Power Systems, 2019, vol. 34, no. 2, pp. 1610-1619. Available: 10.1109/tpwrs.2018.2877743.
- [101] R.E. Macey, "*Hawkeye Line Inspections -Nkonka Idwala No 1 -132kV*", Mace Technologies, Report No. LIM 0802/1, 2008, pp 44-46. [Online]. Available: <https://hyperwave.eskom.co.za> [Accessed: 06- Jan-2020].

- [102] Weather spark, "*Climate and Average Weather Year-Round in Scottburgh*", 2022. [Online]. Available: <https://weatherspark.com/y/96286/Average-Weather-in-Cape-Town-South-Africa-Year-Round>. [Accessed: 07- Mar- 2022].
- [103] SANS 61284:1997, "*Overhead lines - Requirements and tests for fittings*".
- [104] R. Ricker, "*Analysis of pipeline steel corrosion data from NBS (NIST) studies conducted between 1922-1940 and relevance to pipeline management*", Journal of Research of the National Institute of Standards and Technology, 2010, vol. 115, no. 5, p. 373. Available: 10.6028/jres.115.026,
- [105] R. Melchers, "*Bi-modal trend in the long-term corrosion of aluminium alloys*", Corrosion Science, 2014, vol. 82, pp. 239-247. Available: 10.1016/j.corsci.2014.01.019.
- [106] J. Calitz, "*Conductor and Earthwire Evaluation- Eskom National 2000-2016*", Eskom Resource and Strategy Division- Materials, Chemical, Environmental and Mechanical (MCEM), 2018. [Online]. Available: <https://hyperwave.eskom.co.za> [Accessed: 06- Jan- 2022].
- [107] IEC 888:1987, "*Zinc-coated steel wires for stranded conductor*".
- [108] IEC 889:1987, "*Hard-drawn aluminium wire for overhead line conductors*".
- [109] Weather Spark, "*Climate and Average Weather Year-Round in Worcester South Africa*", 2022. [Online]. Available: <https://weatherspark.com/y/84216/Average-Weather-in-Worcester-South-Africa-Year-Round>. [Accessed: 07- Mar- 2022].
- [110] Weather Spark, "*Climate and Average Weather Year-Round in Cape Town South Africa*", 2022. [Online]. Available: <https://weatherspark.com/y/82961/Average-Weather-in-Cape-Town-South-Africa-Year-Round>. [Accessed: 07- Mar- 2022].
- [111] Weather Spark, "*Climate and Average Weather Year-Round in Mandini South Africa*", 2022. [Online]. Available: <https://weatherspark.com/y/96785/Average-Weather-in-Mandini-South-Africa-Year-Round>. [Accessed: 07- Mar- 2022].
- [112] Weather Spark, "*Climate and Average Weather Year-Round in Mpumalanga South Africa*", 2022. [Online]. Available: <https://weatherspark.com/y/96295/Average-Weather-in-Mpumalanga-South-Africa-Year-Round>. [Accessed: 07- Mar- 2022].

- [113] Weather Spark, "*Climate and Average Weather Year-Round in Hluhluwe South Africa*", 2022. [Online]. Available: <https://weatherspark.com/y/97164/Average-Weather-in-Hluhluwe-South-Africa-Year-Round>. [Accessed: 07- Mar- 2022].
- [114] Weather Spark, "*Climate and Average Weather Year-Round in Kraaifontein South Africa*", 2022. [Online]. Available: <https://weatherspark.com/y/82959/Average-Weather-in-Kraaifontein-South-Africa-Year-Round>. [Accessed: 07- Mar- 2022].
- [115] Weather Spark, "*Climate and Average Weather Year-Round in AFB Langerbaanweg South Africa*", 2022. [Online]. Available: <https://weatherspark.com/y/148408/Average-Weather-in-AFB-Langerbaanweg-South-Africa-Year-Round>. [Accessed: 07- Mar- 2022].
- [116] J. Calitz, "*Boskloof- Tousrivier -132 kV line – Wolf Conductor Evaluation*", Eskom Resource and Strategy Division- Materials, Chemical, Environmental and Mechanical (MCEM), Report No. RTD/MAT/14/331, 2014. [Online]. Available: <https://hyperwave.eskom.co.za> [Accessed: 06- Jan- 2022].
- [117] J. Calitz, "*Dassenberg- Koeburg 66kV Line- Conductor and Shield wire Evaluation*", Eskom Resource and Strategy Division- Materials, Chemical, Environmental and Mechanical (MCEM), Report No. RTD/MAT/15/196, 2015. [Online]. Available: <https://hyperwave.eskom.co.za> [Accessed: 06- Jan- 2022].
- [118] J. Calitz, "*Grassridge- Kudu 132 kV line – Shield and Phase conductor Evaluation*", Eskom Research and Innovation Division- Materials Technology, Report No. ERID/MAT/07/2311, 2007. [Online]. Available: <https://hyperwave.eskom.co.za> [Accessed: 06- Jan- 2022].
- [119] J. Calitz, "*Grassridge- Kudu 132 kV line – Shield and Phase conductor Evaluation*", Eskom Research and Innovation Division- Materials Technology, Report No. ERID/MAT/07/2311, 2007. [Online]. Available: <https://hyperwave.eskom.co.za> [Accessed: 06- Jan- 2022].
- [120] J. Calitz, "*Mechanical and Material Evaluation of a Wolf Conductor Sample from Georgedale Abattior No. 1 132kV Line*", Eskom Research and Innovation Division- Materials Technology, Report No. ERID/MAT/07/218, 2007. [Online]. Available: <https://hyperwave.eskom.co.za> [Accessed: 06- Jan- 2022].
- [121] J. Calitz, "*Corrosion Investigation of a Wolf Conductor Sample from the Impala- Pongola 132kV Line*", Eskom Research and Innovation Division- Materials Technology, Report No. TRRIS971087, 2007. [Online]. Available: <https://hyperwave.eskom.co.za> [Accessed: 06- Jan- 2022].

- [122] J. Calitz, "*Stikland- Bluedowns No. 2 132 kV Line – Bear conductor Evaluation*", Eskom Resource and Strategy Division- Materials, Chemical, Environmental and Mechanical (MCEM), Report No. RTD/MAT/15/325, 2015. [Online]. Available: <https://hyperwave.eskom.co.za> [Accessed: 06- Jan- 2022].
- [123] M. Salojee, "*Kerschbosch- Moorreesburg 132 kV Line – Bear Phase conductor Evaluation*", Eskom Resource and Strategy Division- Materials, Chemical, Environmental and Mechanical (MCEM), Report No. RTD/MAT/18/181, 2018. [Online]. Available: <https://hyperwave.eskom.co.za> [Accessed: 06- Jan- 2022].
- [124] Weather Spark "*Climate and Average Weather Year-Round in Saldanha South Africa*", 2022. [Online]. Available: <https://weatherspark.com/y/81931/Average-Weather-in-Saldanha-South-Africa-Year-Round>. [Accessed: 07- Mar- 2022].
- [125] Weather Spark, "*Climate and Average Weather Year-Round in Hendrina South Africa*", 2022. [Online]. Available: <https://weatherspark.com/y/95837/Average-Weather-in-Hendrina-South-Africa-Year-Round>. [Accessed: 07- Mar- 2022].
- [126] Weather Spark, "*Climate and Average Weather Year-Round in Stellenbosch South Africa*", 2022. [Online]. Available: <https://weatherspark.com/y/82954/Average-Weather-in-Stellenbosch-South-Africa-Year-Round>. [Accessed: 07- Mar- 2022].
- [127] Weather Spark, "*Climate and Average Weather Year-Round in Grahamstown South Africa*", 2022. [Online]. Available: <https://weatherspark.com/y/92833/Average-Weather-in-grahamstown-South-Africa-Year-Round>. [Accessed: 07- Mar- 2022].
- [128] Weather Spark, "*Climate and Average Weather Year-Round in Bhisho South Africa*", 2022. [Online]. Available: <https://weatherspark.com/y/94165/Average-Weather-in-Bhisho-South-Africa-Year-Round>. [Accessed: 07- Mar- 2022].
- [129] Weather Spark, "*Climate and Average Weather Year-Round in Cape Town International Airport South Africa*", 2022. [Online]. Available: <https://weatherspark.com/y/148407/Average-Weather-in-Cape-Town-International-Airport-South-Africa-Year-Round>. [Accessed: 07- Mar- 2022].
- [130] Weather Spark, "*Climate and Average Weather Year-Round in Kraaifontein South Africa*", 2022. [Online]. Available: <https://weatherspark.com/y/82959/Average-Weather-in-Kraaifontein-South-Africa-Year-Round>. [Accessed: 07- Mar- 2022].

- [131] J. Calitz, “*Dassenberg - Koeberg 66kV line –Conductor and Hardware Evaluation*”, Eskom Resource and Strategy Division- Materials, Chemical, Environmental and Mechanical (MCEM), report No. RTD/MAT/15/196, 2015. [Online]. Available: <https://hyperwave.eskom.co.za> [Accessed: 06- Jan- 2020].
- [132] J. Calitz, “*Evaluation of Steel shield wire from the Kudu- Melkhout 132kV Line*”, Eskom Resource and Strategy Division- Materials, Mechanical and Civil Technology, Report No. TRR/S01/075, 2001. [Online]. Available: <https://hyperwave.eskom.co.za> [Accessed: 06- Jan- 2020].
- [133] J. Calitz, “*Mechanical and material evaluation of a Goat conductor from Acacia - Platteklouf 132 kV line*”, Eskom Resource and Strategy Division- Materials, Chemical, Environmental and Mechanical (MCEM), 2013. [Online]. Available: <https://hyperwave.eskom.co.za> [Accessed: 06- Jan- 2020].
- [134] J. Calitz, “*Aurora-Kerschbosch 132 kV line – Steel Shield wire evaluation*”, Eskom Resource and Strategy Division- Materials, Chemical, Environmental and Mechanical (MCEM), report No. RTD/MAT/16/155, 2016. [Online]. Available: <https://hyperwave.eskom.co.za> [Accessed: 06- Jan- 2022].
- [135] M. Salojee, “*Henrina 132kV Shield wire Failure Investigation*”, Eskom Resource and Strategy Division- Materials, Chemical, Environmental and Mechanical (MCEM), report No. RTD/MAT/18/252, 2018. [Online]. Available: <https://hyperwave.eskom.co.za> [Accessed: 06- Jan- 2022].
- [136] J. Calitz, “*Grassridge- Kudu 132 kV line – Shield and Phase conductor Evaluation*”, Eskom Research and Innovation Division- Materials Technology, report No. ERID/MAT/07/2311, 2007. [Online]. Available: <https://hyperwave.eskom.co.za> [Accessed: 06- Jan- 2022].
- [137] J. Calitz, “*Mechanical and Material Evaluation of a Shield wire Sample from the Buffalo Prembroke N0.3 132kV Line*”, Eskom Research and Innovation Division- Materials Technology, report No. ERID/MAT/08/2440, 2008. [Online]. Available: <https://hyperwave.eskom.co.za> [Accessed: 06- Jan- 2022].
- [138] M. Salojee, “*Belville South- Triangle 66kV Line- Steel Shield wire Evaluation*”, Eskom Resource and Strategy Division- Materials, Chemical, Environmental and Mechanical (MCEM), report No. RTD/MAT/18/127, 2018. [Online]. Available: <https://hyperwave.eskom.co.za> [Accessed: 06- Jan- 2022].
- [139] M. Salojee, “*Stikland- Oakland 66kV Line- Steel Shield wire Evaluation*”, Eskom Resource and Strategy Division- Materials, Chemical, Environmental and Mechanical (MCEM), report No. RTD/MAT/18/128, 2018. [Online]. Available: <https://hyperwave.eskom.co.za> [Accessed: 06- Jan- 2022].